UNIVERSITÀ DEGLI STUDI DI PADOVA

Dipartimento di Ingegneria Industriale DII

Corso di Laurea Magistrale in Ingegneria Energetica

DESIGN AND OPTIMIZATION OF SELF-RECTIFYING

WIND TURBINES

Relatore: Prof. Giorgio Pavesi
Supervisor: Prof. Antoine Dazin
Co-Supervisor: Prof. Annie-Claude Bayeul-Lainé

Laureando
Alberto Baretter   1129089

Anno Accademico 2017-2018

CONTENTS

INTRODUCTION

The present master thesis work concentrates on the design and optimization of self-rectifying turbines for a possible energy recovery application in the Channel Tunnel.

Self rectifying turbines are, by definition, special types of turbines that rotate in the same direction irrespective of the flow direction. Looking at figure (0.1), this means that whether the flow is coming from positive z direction or negative z direction, the turbine rotates in the x-y plane always in couterclock-wise direction.
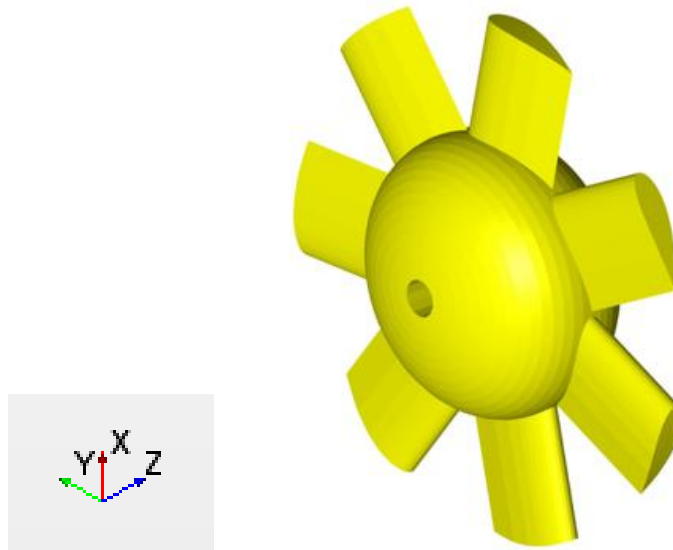

Fig. 1-1:geometry of Wells self-rectifying turbine

This special requirement has been used traditionally to extract energy from sea and ocean waves through OWC (oscillating water column) plants. In figure (0.2) the main idea of an OWC is represented. Water waves create compression and decompression of an air column which can be directed into an air turbine to generate electricity. Air as a working fluid instead of salty water avoids of course corrosion problems on the blades and the casing.
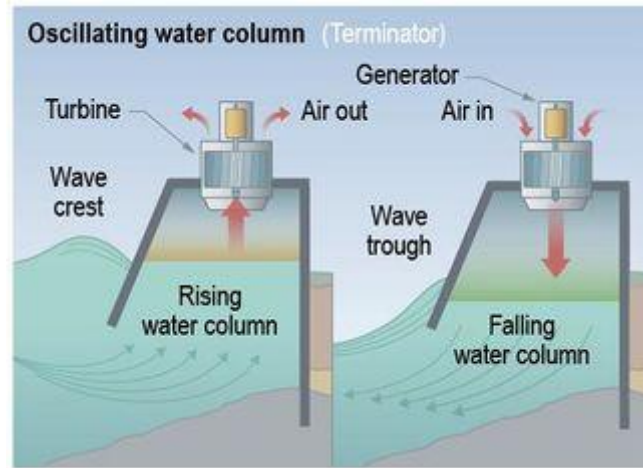
Fig. 1-2: oscillating water column power plant

The possible application which is considered in this work deals only with air: inside Channel Tunnel trains are creating a strong piston effect and a lot of viscous friction dissipation on the tunnel walls, especially in the transverse tunnels (piston relief ducts) in (fig.0.3) ,which are partially closed by some diaphragms which act as valves introducing a pressure drop. These diaphragms had been installed to reduce the pressure at the outlet of the pressure relief ducts to reduce forces acting on trains sides.

The trains tunnel and transverse ones are represented in figure (0.3). The whole channel is 50 km long, with transverse tunnels every 250 m. In figure (0.4) a representation of the diaphragms is given.
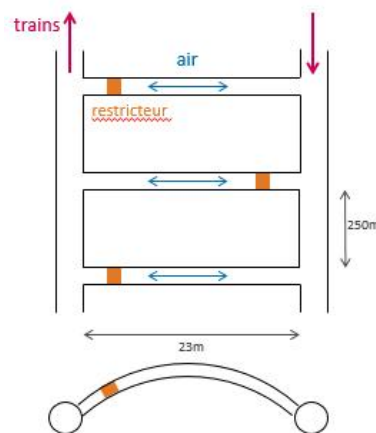

Fig. 1-3: Scheme of channel tunnel

Fig. 1-4: Picture of diaphragms in the transverse channels

Because of friction dissipation and of course also trains electric motors heating, a lot of heat is generated (2MW estimated for the whole 50 km tunnel), and the temperature inside the tunnels must be kept into acceptable range with the help of refrigerating systems which are expensive.

A possible energy recovery intervention could be the replacement of the diaphragms with self-rectifying turbines in order to recover a part of the kinetic energy of the air streams in the transverse tunnels. Turbines can create the same pressure drop that diaphragms are creating, but they will produce electrical energy. With such a system not only electrical energy for tunnel illumination can be produced, but heat production is also reduced with benefits to the refrigerating systems that can consume less power to keep required temperature.

More specific details about the heat loads in the tunnels and possible estimated energy recovery can be found in the reference [1].

For this application, two axial turbines have been considered and compared:

-Wells turbine

-Impulse turbine

For each of them an optimized design is proposed, with the help of the CFD Software Star-CCM+. Having a design for each turbine helps the comparison, and finally helps to choose which of the two turbines could be the best solution for this application.

The design of the two turbines done in this work is based on steady state calculation, as a starting point, neglecting the various dynamical effects related to wind moving in the tunnel and starting characteristics of the turbines. Despite the strong dynamical effects created by air flowing the tunnels, steady state calculations are very useful at a design stage because it has been shown that quasi-steady calculations can be applicable to OWC systems with irregular wave motion [2] [3].

The procedure used for design is the following:

-preliminary design based on mean radius 1D calculations done in Matlab,

-2D validation of preliminary design at mean radius with CFD calculations in Star-CCM+

The best solution is the one that maximizes efficiency; no economic considerations have been made at this point of the project.

The definition of the efficiency on which the comparison has been made comes from an energy balance across the turbine; power is extracted by the machine at the expense of kinetic and pressure energy of the flow. In the process some power P_{diss} is dissipated due to the friction.

$$\frac{1}{2}\dot{m}(v_{in}^2 - v_{out}^2) + \dot{m}\frac{p_{in} - p_{out}}{\rho} = P_{diss} + P_{mecc}$$

Efficiency is defined as :

$$\eta = \frac{P_{mecc}}{P_{diss} + P_{mecc}}$$

which is

$$\eta = \frac{P_{mecc}}{\frac{1}{2}\dot{m}(v_{in}^2 - v_{out}^2) + \dot{m}\frac{p_{in} - p_{out}}{\rho}}$$

And since total pressure is defined as:

$$p_0 = p + \frac{1}{2}\rho v^2 \qquad (0.1)$$

$$\eta = \frac{P_{mecc}}{\dot{m}\dfrac{p_{0\_in} - p_{0\_out}}{\rho}}$$

And if Q is the volumetric flow rate,

$$\eta = \frac{P_{mecc}}{Q \cdot \Delta p_0} \qquad (0.2)$$

This work is organized in the following way:

In the first chapter, experimental air flow velocity and pressure data inside the tunnels [1] are reported, and the project specifications are presented.

In the second chapter, a 1D model for Wells turbine is developed, based on momentum and blade element theory, to propose a preliminary design. Then, a 2D model in StarCCM+ is developed to validate the preliminary design.

In the third chapter, a 1D model for Impulse turbine is developed, based on pressure drop correlations found in literature [4], [5], [6] [7] and a preliminary design is proposed. In a second moment, a 2D model in StarCCM+ is developed to validate the preliminary design.

In the last chapter, a comparison between the two turbines is done , based on the 2D validated models, and advantages and disadvantages of both solutions are presented.

1 PROJECT SPECIFICATIONS :

The specifications based on which the project is developed are:

-pressure drop imposed by the diaphragms that have to be substituted: 1000 Pa +/- 5%.

-external diameter of machine, imposed by the diameter of the transversal tunnel: 2 m.

- air flow axial velocity v=20 m/s.

The choice of design pressure drop and air flow velocity are related to the velocity and pressures which are developed in the pressure relief ducts as a consequence of trains moving;

In (fig. 1.1) velocity conditions at the inlet of the turbine are represented. These velocities are imposed by velocity of trains passing in the tunnel, time interval between trains, tunnels geometry. By experiments some pressure and velocity data in the transverse tunnel have been found:
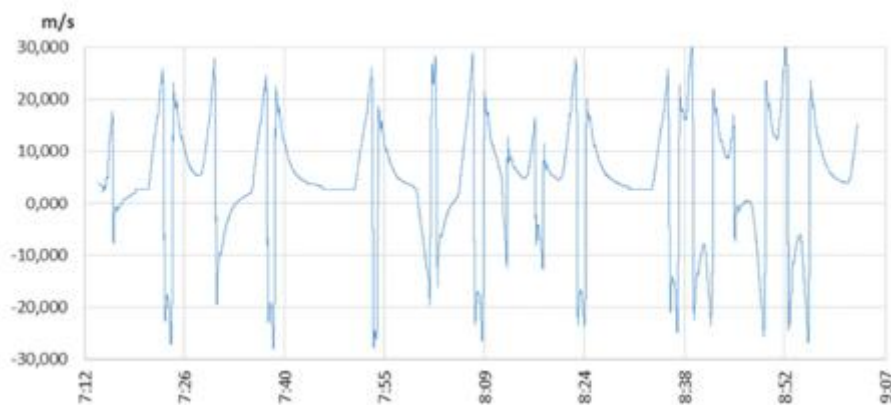

Fig. 1-1: velocity in the middle of transverse tunnel as a function of time in a range of 2 hours; taken form [1]

Since the turbine is self-rectifying, all velocities were assumed positive In (fig.1.2) the modulus of velocities is represented.
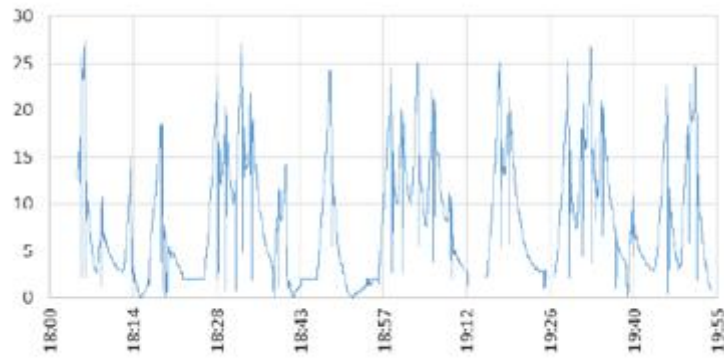
Fig. 1-2: modulus of velocities in figure 1.26; taken from [1]

In figure (1.3) the pressure drop measured in the middle of the pressure relief duct during the same time interval of 2 h , is shown.
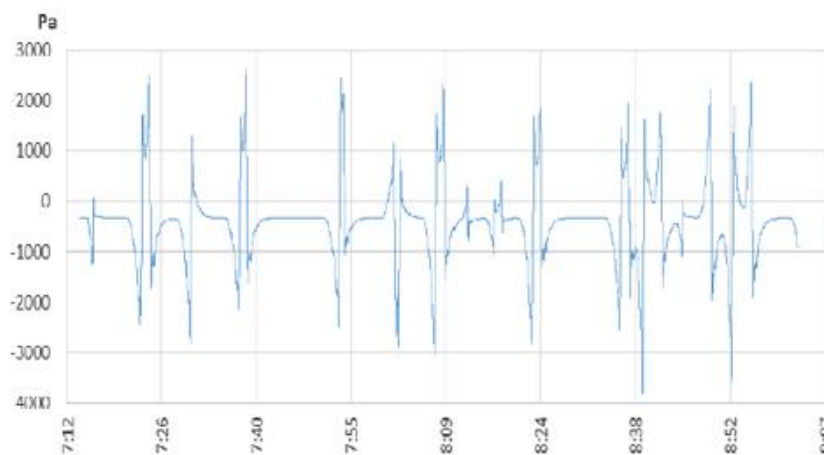

Fig. 1-3: pressure drop measured in the middle of the tunnel; taken from [1]

Velocity profile is heavily irregular and unsteady, with strong gradients. There are some time intervals in which velocity seems to reach steady state, around a value of 3 m/s and the corresponding pressure drop reaches a value of 300 Pa.

The choice of the v velocity at design point, for which the turbine should operate with best efficiency, could be based on energy production capability of the site calculated from power density (DP) [W/m^2].

Power density is the power extracted by the turbine per unit cross sectional area; the power extracted by a wind turbine can be thought as a fraction of the power contained in the incoming wind. This can be expressed as:

$$P = c_p \cdot \frac{1}{2} \cdot \dot{m} \cdot v^2$$

where the coefficient c_p contains all the specific characteristics of the machine and makes the difference between Impulse turbine and Wells turbine.

Since mass flow rate is:

$$\dot{m} = \rho \cdot A \cdot v$$

the power becomes:

$$P = c_p \cdot \frac{1}{2} \cdot \rho \cdot A \cdot v^3 \qquad (1.1)$$

and the power density:

$$DP = c_p \cdot \frac{1}{2} \cdot \rho \cdot v^3 \qquad (1.2)$$

As it is seen from equation (1.1) the higher the velocity in the tunnel is, the higher the power extracted is, but high velocities in the tunnel are non-frequent, as seen from (fig. 1.1). Consistently if a high axial velocity like is chosen to design the turbine with maximum efficiency right for 25 m/s it will operate at design condition very unfrequently and even if high power will be extracted at design condition the energy extracted will be low.

Likewise, it is a good idea to design for a low velocity like 5 m/s. These velocities are very frequent but the corresponding instantaneous power extracted won't be as high as for 25 m/s.

It is expected there is a condition in between these two in which the product of power and time is maximum, and energy extracted is maximum.

Specific Energy [J/m^2] that is produced by running the turbine is:

$$\int DP \cdot dt \qquad \qquad (1.3)$$

To solve the integral for velocity, a change of variable from time to velocity is done:

first, from (fig.1.1) the percentage of time over the total range of 2 h in which a certain velocity is present in the tunnel is derived, and plotted in (fig.1.4). The plot indicates for every velocity, the time that velocity is present in the tunnel in the range of 2 h chosen.
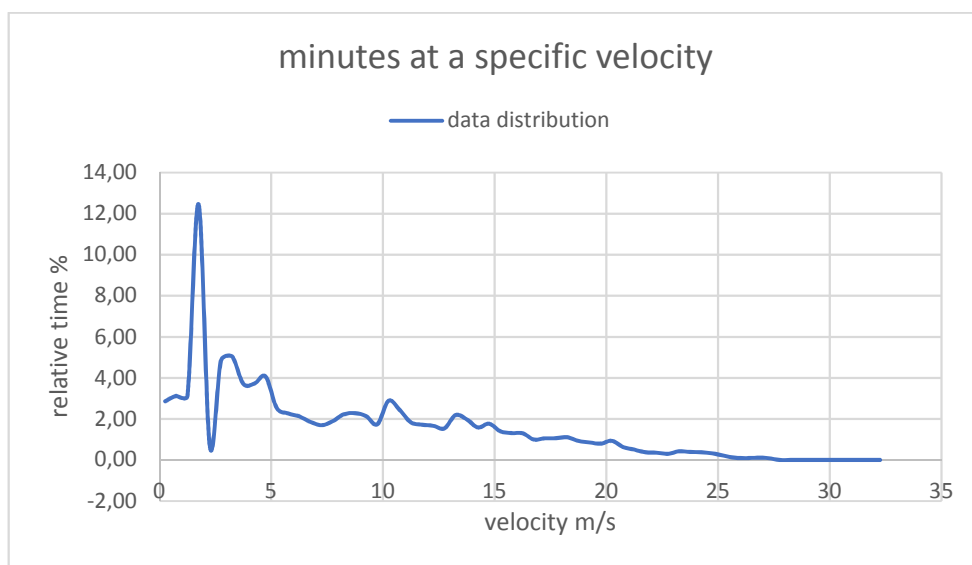

Fig. 1-4: Percentage of time a certain velocity is present in the pressure relief duct

It is possible to express this data distribution with a continuous function f(v) called Weibull distribution function which is shown in (fig. 1.5)
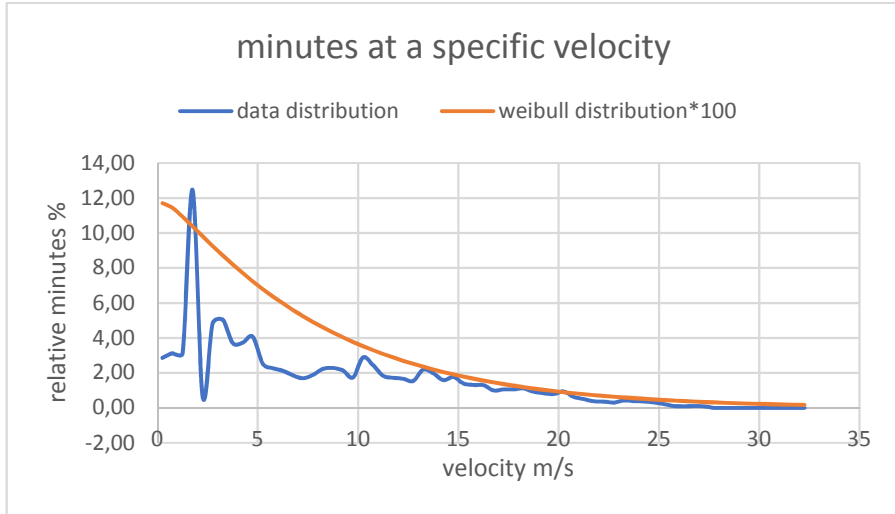
Fig. 1-5: Weibull distribution of the wind in the tunnel

The integral in (1.3) becomes:

$$\Delta t \cdot \int DP(v) \cdot f(v) \cdot dv \qquad (1.4)$$

where Δt represents the whole time interval of 2h.

Just to show how the calculation works let's imagine a constant c_p coefficient of 0.4. This is a reasonable mean value for wind turbines [8] but it is not constant for different velocities. If it is assumed constant for simplicity, power density is shown in (fig 1.6), and the product of Weibull distribution and power density in (fig.1.7). To represent them both in the same plot, the Weibull distribution has been multiplied by 100.
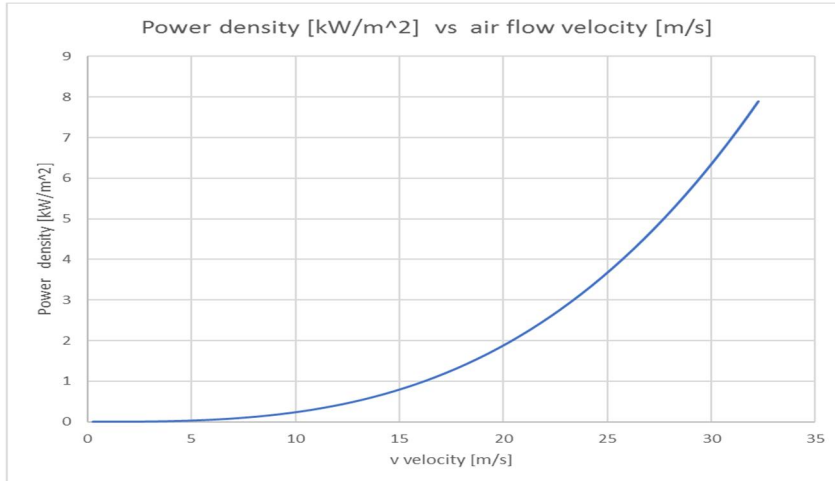
11

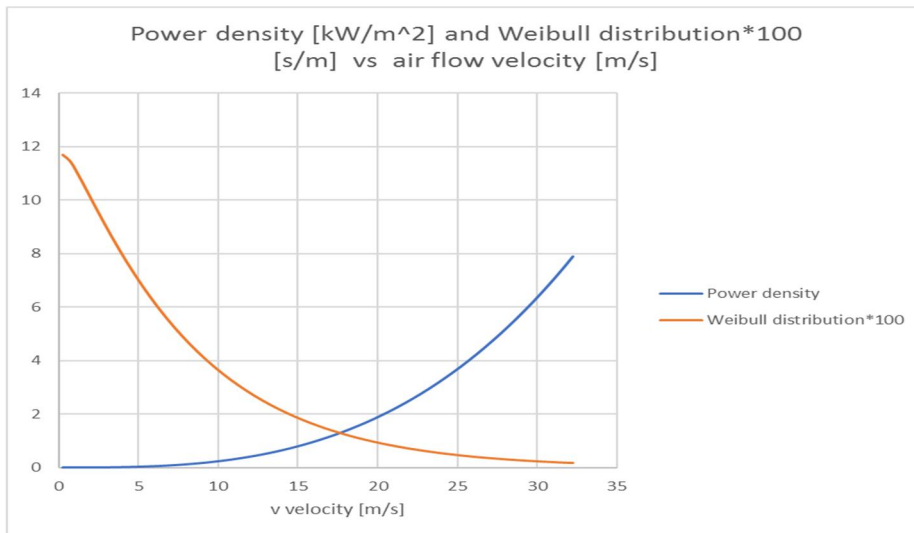*Fig. 1-6: power density that can be extracted by the turbine*

*Fig. 1-7: power density and Weibull distribution *100*

The product of DP and f(v) unit is J/m^3, an energy per unit volume. From the products of the two curves (fig 1.7), one expects low velocities to result in poor power extraction even if they are very frequent. High velocities have favourable power extraction but are less frequent. In both cases energy extracted won't be high.

A velocity, which contributes more than all the others to energy production, is expected: from the product of the two curves, one can find the velocity at which this maximum occurs (fig 1.8).
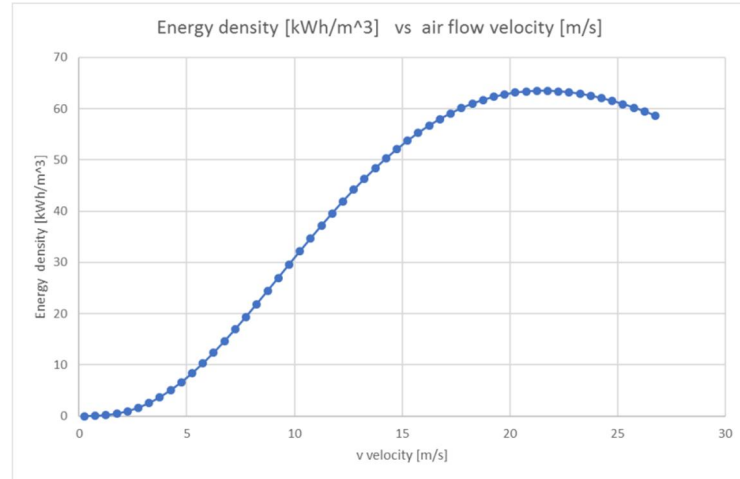
Fig. 1-8: Energy density that can be extracted by a constant 0.4 cp , in the pressure relief duct

With the assumption made on c_p ,to produce maximum energy, design velocity should chosen at 22 m/s. Of course however, c_p is not constant and it depends on the type of turbine. An energy production calculation has been made in [1] using c_p of a real Wells turbine and the velocity is chosen at 20 m/s.

As far as the pressure drop is concerned, it would be desirable that the behaviour of the turbines in term of pressure drop is similar to the behaviour of diaphragms:

the pressure drop developed by the diaphragms can be modelled in steady state by an equation of the type:

$$\Delta p = k \cdot \frac{1}{2} \cdot \rho \cdot v^2 \qquad (1.5)$$

But the actual relationship between the pressure drop and the velocity that could be built from (fig 1.1) and (fig 1.3), is far from (1.5) because an inertial term due to unsteady behaviour is present:

$$\Delta p = k \cdot \frac{1}{2} \cdot \rho \cdot v^2 + \rho \cdot L \cdot \frac{dv}{dt}$$

L is the length of the pressure relief duct.

The inertial term is difficult to determine and it makes very difficult to characterize the diaphragm in terms of a k constant, and so to find a couple of values for velocity and pressure that could be taken for the design of the turbines.

Anyway from (fig 1.3) it can be seen that values of pressure drop are exceeding 1000 Pa only at the moment when the train is just passing in correspondence of the pressure relief duct, and this value of pressure is present just for seconds, before the pressure falls and starts oscillating. So it will be reasonable to choose a value of 1000 Pa +/- 5% for the pressure drop that the turbines should develop at design conditions.

In this brief chapter the specifications and constraints for the project have been shortly discussed; in the next chapter a design for Wells turbine will be proposed, based on the specifications discussed in this chapter.

2 WELLS TURBINE

In this chapter, the design of the Wells turbine is carried out: first blade element theory and momentum theory are presented, as they are the theoretical foundations to build a 1D model of the machine in a Matlab code. Then are presented the typical power and efficiency curves for Wells turbine calculated with Matlab code for one specific geometry of 0.1 m chord length and 8 number of blades (reasonable values found in literature [9]) chosen as an illustrative example. After that, the optimization performed by Matlab code is described, and the best configuration is proposed. A 2D validation of the model follows; some CFD simulations are performed in a narrow range around the design parameters found by 1D calculations and finally the optimal parameters for the Wells turbine according to the 2D model are presented.
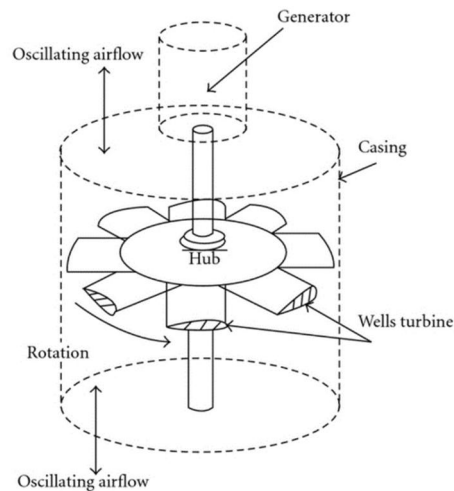

Fig. 2-1: Wells turbine scheme; taken from[oastalenergyandenvironment.web.unc.edu]

Wells turbine (fig.2.1) is an axial flow turbine consisting in an impeller fitted with symmetrical airfoils set radially with a 90° stagger angle, in order to meet the symmetry of the flow constraint. The turbine must in fact behave the same way whether the flow in the figure comes from the bottom or from the top.

One of the system using Wells turbine has been operational in the LIMPET system in Hebrides (UK) as a OWC power plant [10].

A good reference for Wells turbine, that contains a procedure to design the turbine, is [11]

The simplest idea to estimate the performance of turbines is referring to a mean behaviour of the flow approaching the blades at one particular radius in terms of a velocity triangles.
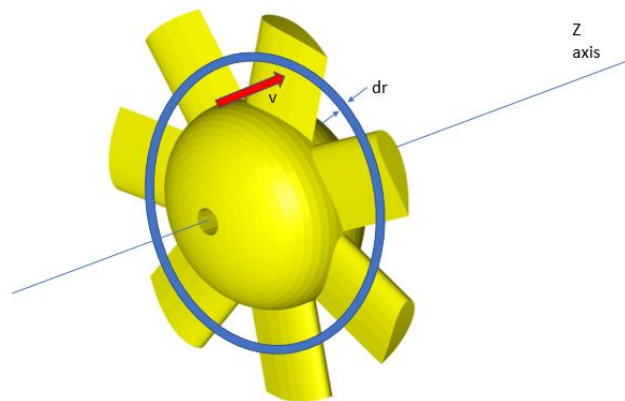

Fig. 2-2: elemental area for 1D design; taken from [A review of Wave to Wire Models for Wave Energy converters, Energies 2016,9(7)]

A small region dr near a specific radius (fig 2.2) is considered and at every tangential position a flow having:

-v, the flow absolute velocity

-w, the flow relative velocity

-u, the blade velocity, related to rotational velocity by u=ω* r

can be identified.

The vectorial sum of blade and relative velocity is always equal to absolute velocity. This representation is called monodimensional, because 2D pressure gradients that happen on tangential direction between two blades, and 3D effects at different radii are neglect. It is also called mean line analysis because it focuses only on one radius.

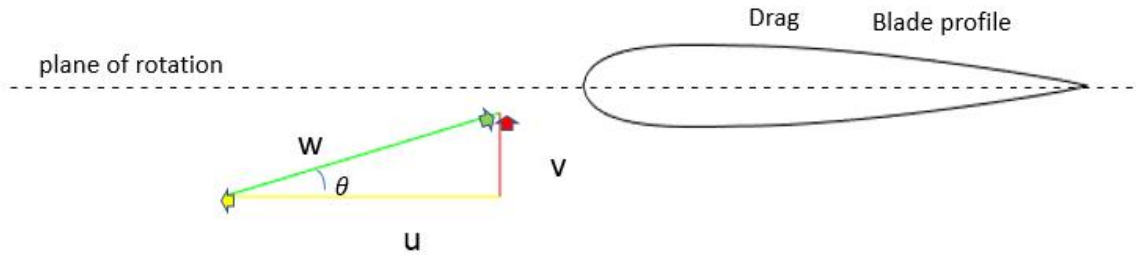In (fig. 2.3) velocity triangles for Wells turbine are represented;

Fig. 2-3: triangle of velocities at the inlet

The air flow in the tunnel is coming with an absolute velocity v and the turbine is rotating with a tangential velocity u, so the relative velocity enters the turbine with an angle θ with respect to the blade profile, which is called the angle of attack.

2.1 BLADE ELEMENT THEORY:

When the relative current enters in contact with the profile, two forces are created as a result of the pressure and velocity fields that develop around the airfoil: lift force and drag force.

These forces are proportional to the profile area and to the relative dynamic pressure according to coefficients called lift and drag coefficients that are complex functions of geometry of the airfoil, Reynolds number and angle of attack.

$$Lift = c_l \cdot A \cdot \frac{1}{2} \rho \, w^2 \qquad\qquad (2.1)$$

$$Drag = c_d \cdot A \cdot \frac{1}{2} \rho \, w^2 \qquad\qquad (2.2)$$

The area represented by A, in the model is

$$A = c \cdot dr$$

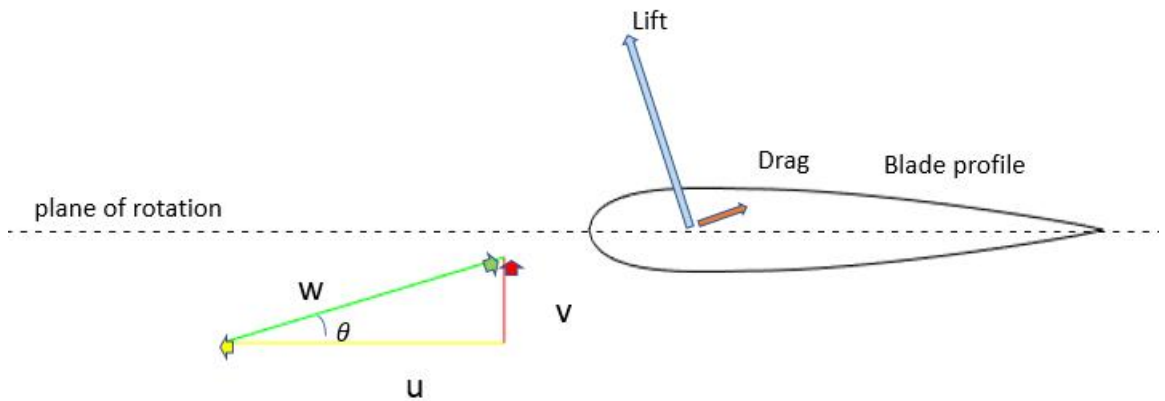having called c the chord of the airfoil. The two forces are represented in (fig 2.4)

Fig. 2-4: Developed lift and drag forces

When the two vectors are decomposed on tangential and axial directions, two other forces are obtained (fig.2.5): thrust and tangential force F, the last one being responsible of creating the torque, and thus the power.
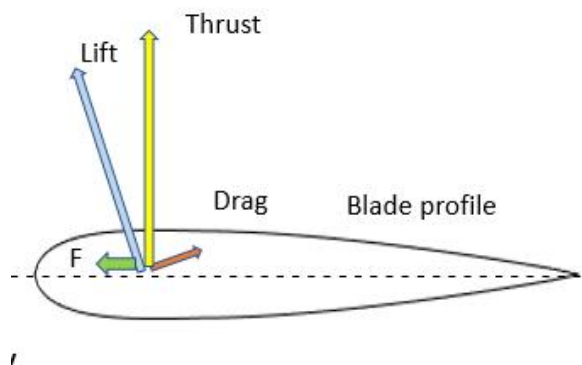

Fig. 2-5:thrust and tangential force F

$$Thrust = Lift \cdot cos(\theta) + Drag \cdot sin(\theta) \tag{2.3}$$

$$F = Lift \cdot \sin(\theta) - Drag \cdot \cos(\theta) \tag{2.4}$$

By substituting Lift expression into F:

$$F = [c_l \cdot \sin(\theta) - c_d \cdot \cos(\theta)] \cdot A \cdot \frac{1}{2}\rho w^2$$

Collecting all the terms related to force coefficients into Cy

$$F = c_y \cdot A \cdot \frac{1}{2}\rho w^2 \tag{2.5}$$

Power produced is related to torque T by multiplying it by the angular velocity and the number of blades nb.

$$T = r \cdot c_y \cdot A \cdot \frac{1}{2}\rho w^2 \tag{2.6}$$

$$P = n_b \cdot \omega \cdot r \cdot c_y \cdot A \cdot \frac{1}{2}\rho w^2 \tag{2.7}$$

In an analogous way we can derive an expression for the thrust force:

$$Thrust = [c_l \cdot \cos(\theta) + c_d \cdot \sin(\theta)] \cdot A \cdot \frac{1}{2}\rho w^2$$

and again collecting all the terms related to force coefficients into Cx

$$Thrust = c_x \cdot A \cdot \frac{1}{2}\rho w^2 \tag{2.8}$$

The two forces are strongly related to cy and cx and so by lift and drag coefficients which are usually given for an airfoil after experimental tests. Data are found on NACA archives [http://airfoiltools.com], for example, in form of tables, from which curves can be extrapolated by fitting the points.

For airfoil NACA 0012 for example, curves for lift and drag coefficients are plotted. The coefficients are functions of angle of attack (fig. 2.4) and Reynolds number:

$$Re = \frac{\rho \cdot w \cdot c}{\mu}$$

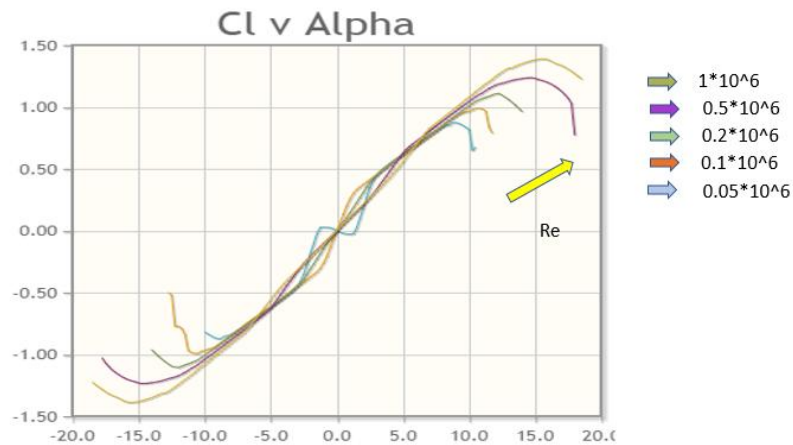which represents the ratio of inertia forces to viscous forces

Fig. 2-6: Lift coefficient as a function of angle of attack and Re number[http://airfoiltools.com]
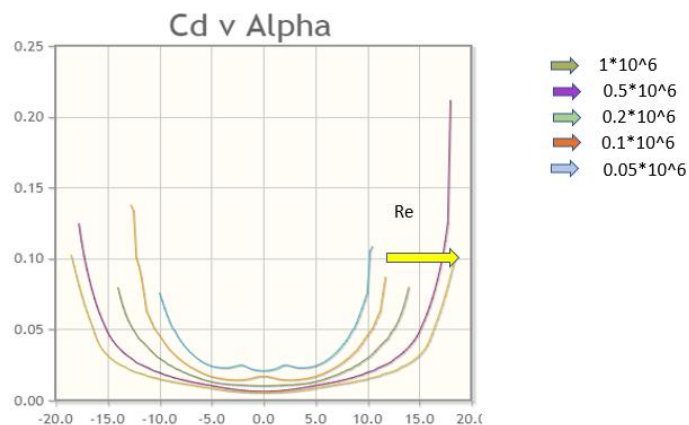

Fig. 2-7: Drag coefficient as a function of angle of attack and Re number [http://airfoiltools.com]

It can be observed in (fig 2.6) that for low values of alpha (around [0°- 3°]) the lift coefficient is low, and so lift force, which is comparable to drag force, with the

20

effect that no positive tangential force will be produced. This is called drag region, as the effect of drag forces created by friction with the airfoil is sufficiently high to prevent the blade to turn.

If the angle of attack is increased, a beneficial effect on lift coefficient it is highlighted, because it increases , more than drag increase, and this increase is almost linear. This is the optimal region to operate the airfoil, since a lift force much higher than the drag force means a higher torque to be developed.

But if the angle of attack is increased towards values of 10° to 18° depending on the Reynolds number, a sudden fall of the lift coefficient is observed while for the same angle, drag coefficient increases dramatically with the consequence that ability to produce torque decreases rapidly. This is due to separation of the flow from the boundary layer which decelerates the flow on the upper surface and re-equilibrates pressures between upper and lower part of the blade reducing lift. The phenomenon is called stall and is represented schematically in fig. (2.8).

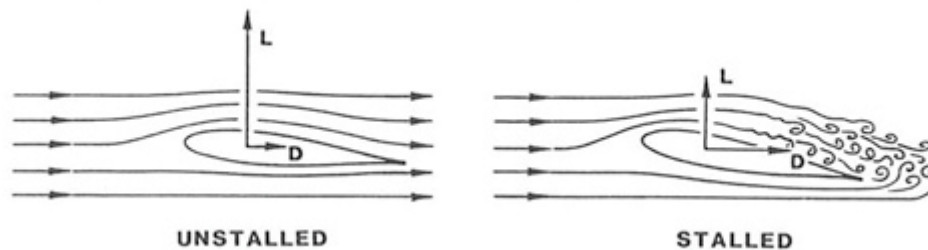UNSTALLED   STALLED

Fig. 2-8: Low angle of attack unstalled blade and higher angle of attack stalled blade; taken from [AVIATION INVESTIGATION REPORT A09Q0210, Transportation safety board of Canada]

It is really important to note that these data are given for an airfoil in a free stream, without other objects around that can disturb the flow, like other blades, so the forces that are calculated using these data are not the correct ones to use for an entire turbine cascade. This is the limitation of the above theory.

This can be intuitively understood with a simple consideration regarding Venturi effect: when the air flow approaches the blades, it finds some blockage due to the presence of the blades, and tends to accelerate in the passages between the blades (fig. 2.9).
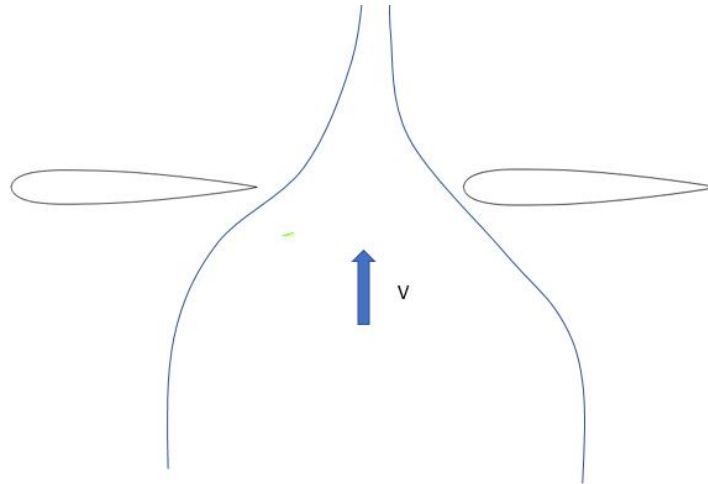
Fig. 2-9: Blockage effect caused by presence of neighbouring blades creates a throat between them

Because of conservation of energy, if the fluid accelerates, the pressure reduces, and these two effects are increased if more blades are present! The number of blades strongly influence the velocity and pressure drop around the airfoil with an effect of the velocity triangles shape (fig. 2.10).
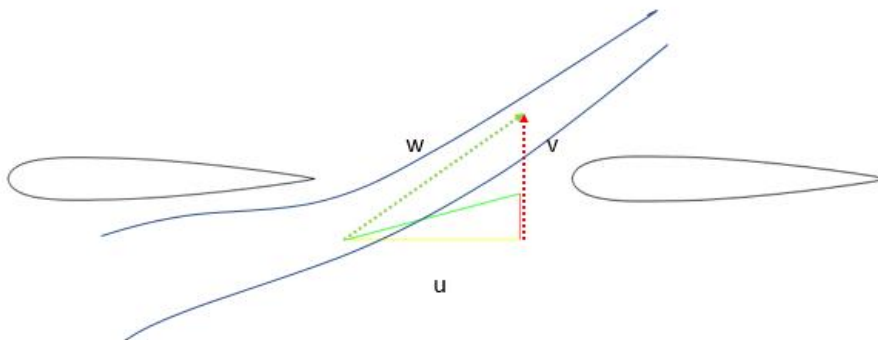

Fig. 2-10: Modification of triangle of velocities due to acceleration of relative current in the throat

Since velocity increases in the throat between the blades, the angle of attack changes, and also the Reynolds number, leading to different lift and drag coefficients.

The parameters affecting the degree of the mutual interference and the problem of the relative steady potential flow of the straight cascade was completely solved by Weinig by conformal mapping. For simplicity it has been chosen to neglect the

effects of the mutual interference in the 1D model, and to use lift and drag coefficients for one blade in free stream as if the blades were far apart each other .

To find an expression for efficiency, according to (0.2) the values of the outlet velocity and the pressure drop have to be known; two conservation laws come into help:

-law of moment of momentum helps finding an expression for tangential velocity at the outlet

-law of axial momentum helps to find an expression for static pressure drop

2.2   MOMENTUM THEORY:

The same two forces lift and drag can be expressed by making use of conservation laws:

at the inlet a certain pressure and an axial momentum are present (fig.2.12); when the fluid encounters the turbine and interacts with it , torque is created and that is done, according to moment of momentum law, with a change in moment of momentum which implies a tangential component of velocity (vt2) to appear at the outlet of the rotor as seen in (fig 2.13).
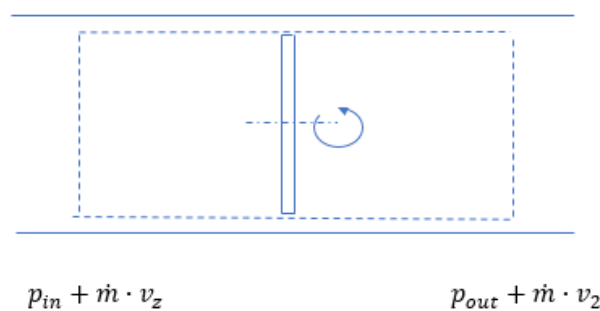

$$p_{in} + \dot{m} \cdot v_z \qquad\qquad p_{out} + \dot{m} \cdot v_2$$

Fig. 2-11: control volume for momentum balance
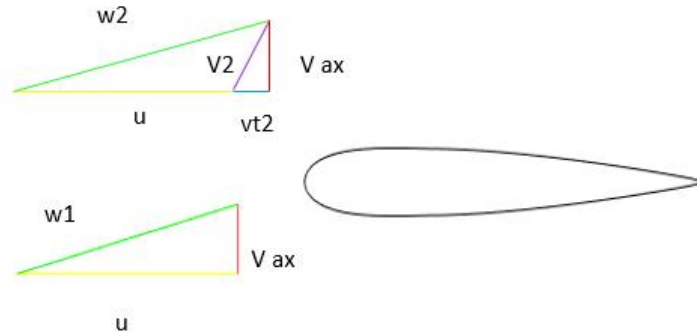
On a small elemental ring law of moment of momentum implies:

$$F \cdot r = (\rho v_d dA) \cdot v_{t2} \cdot r$$

since it is assumed that no change in radial position occur; this is close to reality as the tunnel does not allow an expansion of the wake behind the turbine.

The above equation gives another form for the tangential force:

$$F = \rho v_d 2\pi r \cdot dr \cdot v_{t2}$$

It is common to express the tangential component v_{t2} as a fraction of velocity u through the parameter a' tangential induction factor defined as:

$$\frac{v_{t2}}{u} = \frac{\omega' r}{\omega\, \text{r}} = 2a'$$

$$F = \rho v_z \cdot 2\pi r \cdot dr \cdot 2a'u$$

Setting equal the two expressions found for F we can find out an expression for a'

$$c_y \cdot c \cdot dr \cdot \frac{1}{2}\rho w^2 = \rho v_z \cdot 2\pi r \cdot dr \cdot 2a'u$$

$$a' = \frac{\sigma \cdot c_y}{4 \cdot (\sin \alpha)^2 \cdot \lambda} \tag{2.10}$$

where λ is the tip speed ratio:

$$\lambda = \frac{\omega r}{v_z}$$

Using this expression the velocity at the outlet of the turbine can be estimated, and so efficiency calculated using (0.2).

The tangential induction factor is related to tangential velocity acquired in the wake of the turbine and so of rotational kinetic energy in the wake. This quantity is of great interest since it affects efficiency of the turbine as it will be seen later. Intuitively we are not interested in having high kinetic energy at the outlet of the machine in its wake because it means the machine couldn't transform this amount of energy into work!

From momentum balance in axial direction, always considering the control volume in figure (fig.2.12), since axial component at the inlet and at the outlet are the same:

$$Thrust = (p_{in} - p_{out}) \cdot dA \tag{1.11}$$

or

$$Thrust = n_b \cdot c_x \cdot c \cdot dr \cdot \frac{1}{2}\rho w^2 = 2 \cdot \pi \cdot r \cdot dr \cdot \Delta p$$

where cx is still function of lift , drag coefficient, angle of attack. Pressure drop is:

$$\Delta p = \frac{n_b \cdot c_x \cdot c \cdot \rho w^2}{4 \cdot \pi \cdot r} \tag{2.11}$$

Pressure drop can be written in another form making use of σ solidity which depends on main geometry of the machine:

$$\Delta p = \frac{n_b \cdot c_x \cdot c \cdot \rho w^2}{4 \cdot \pi \cdot r} = \sigma \cdot c_x \cdot \frac{1}{2} \rho w^2$$

Knowing the expressions of power, pressure drop, velocity at the outlet it is possible to estimate the performance of the machine.

2.3   1D PRELIMINARY DESIGN:

Based on the equations developed until this point, a Matlab code has been written to solve the axial and tangential equilibrium. Lift and drag coefficient have been implemented as a function of angle of attack and Reynolds number, so that forces and power can be calculated. The code can perform one calculation at a time, given the number of blades and the chord length, but in order to optimize the design it can also make calculations for different combinations of the number of blades and chord lengths to choose the best solution.

First the code is run for a single configuration of number of blades and chord length (8 blades and 0.1 m chord length) to show typical power and efficiency curves; then the optimization process carried out by the code is described.

In the following, only power and efficiency curves are reported, leaving the results for forces and pressure drop to appendix A.

Two characteristics curves of turbine power production can be calculated:

-Power produced vs rotational velocity

-Power produced vs axial velocity

Turbine characteristics are given in terms of non-dimensional coefficients:

Power coefficient is defined as:

$$c_p = \frac{P}{n_b c \cdot dr \cdot u \cdot \frac{1}{2} \rho w^2} \qquad (2.12)$$

In which the denominator represents all the power of the relative flow that could be extracted. If in (2.12), the numerator P is substituted with (2.7), then

$$c_p = c_y$$

cy was given as a function of the angle of attack, but to express it in terms of u one can remember that:

$$u = \frac{v}{\tan(\theta)} \tag{2.13}$$

If v is fixed, plotting cy as a function of u gives the turbine characteristics for different rotational velocities (fig 2.14).
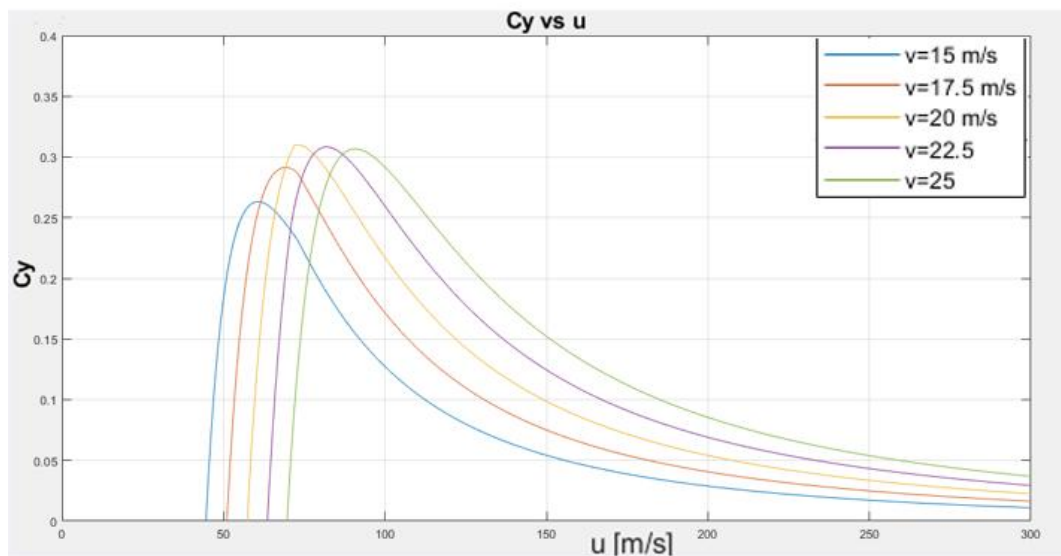

Fig. 2-13: Cy coefficient as a function of u velocity

This characteristic shows that if the value of the axial flow velocity at the turbine inlet is given, the velocity at which the turbine should rotate at design point operation must be chosen carefully because it strongly affects power output and in particular there is a value of u at which maximum power output can be found.

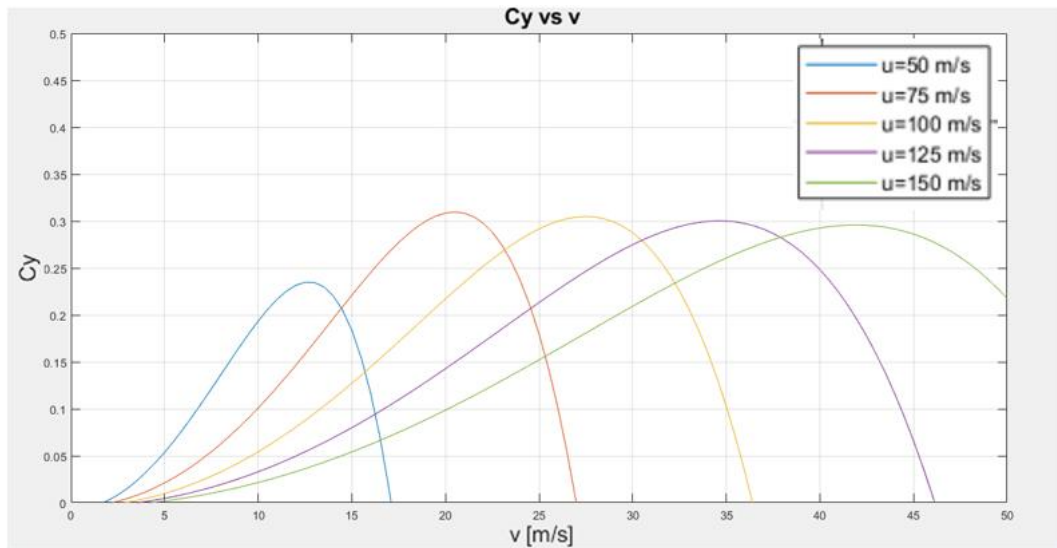For the second characteristic curve, u is fixed and cy is plotted (fig.2.15) as a function of v -equation (2.13)-.

Fig. 2-14: Cy coefficient as a function of v velocity

This characteristic is particularly useful when off-design performance is considered and u is fixed, while air velocity at the inlet is varying. Increasing velocities results in higher power produced, until stall of the blades is reached, and even if velocity v grows, the machine can no more increase power production. It is usual to express the plots as a function of flow coefficient ϕ. (fig.2.16)
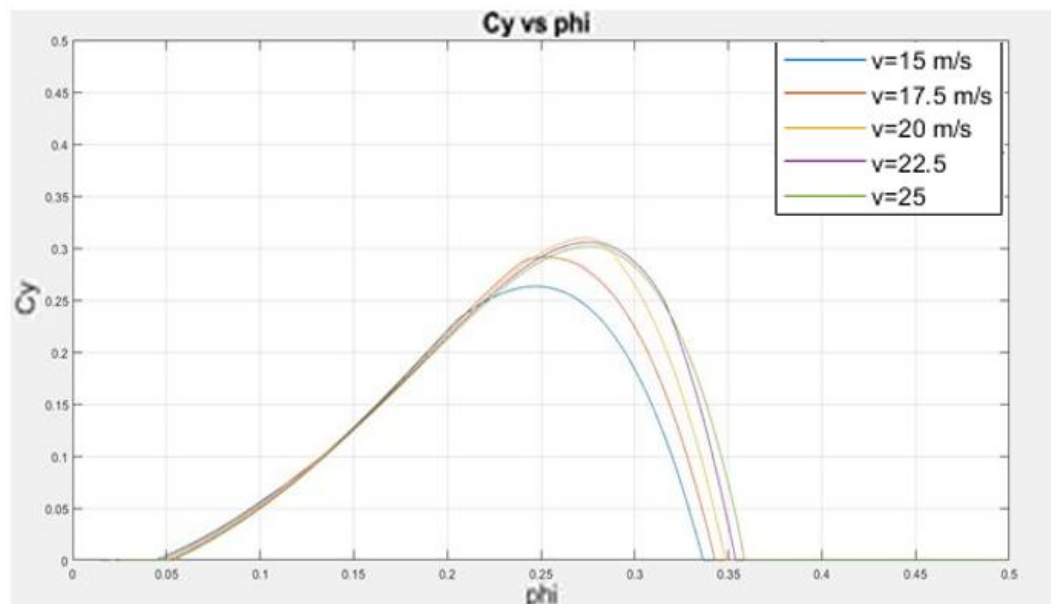
$$\phi = \frac{v}{\omega.r}$$

Fig. 2-15: Cy as a function of phi

Another parameter usually used to describe the turbine performance is efficiency, defined in (0.2) as:

$$\eta = \frac{P_{mecc}}{Q \cdot \Delta p_0}$$

The volumetric flow rate Q [m^3/s] is:

$$Q = v \cdot 2 \cdot \pi \cdot r \cdot dr$$

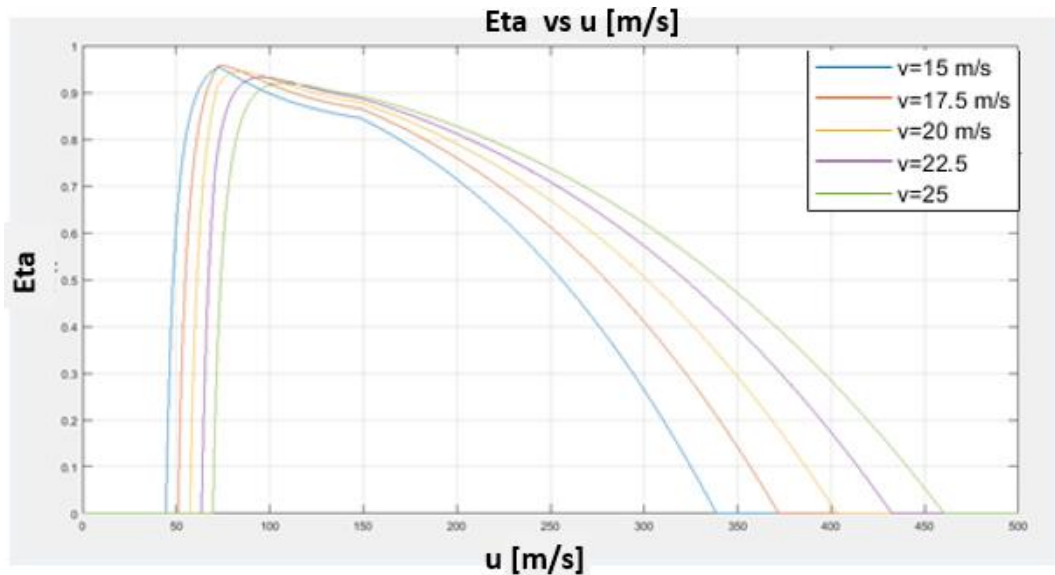In (fig. 2.17) efficiency is plotted as a function of blade velocity.

Fig. 2-16: efficiency as a function of u velocity

Efficiency is very low for tangential velocity u around 60 m/s (fig) because of stalling of the blades. The maximum of efficiency is in the region just before stall, around 80 to 120 m/s and then comes down because of low angle of attack when rotational velocity is high. Velocity u should be limited in this range also because of noise problems. When u is high, usually more than 150 m/s Mach number of 1 could be reached at the leading edge of the blades, and sonic supersonic transition leads to high noise production. In figure (2.18) efficiency is plotted as a function of ϕ.
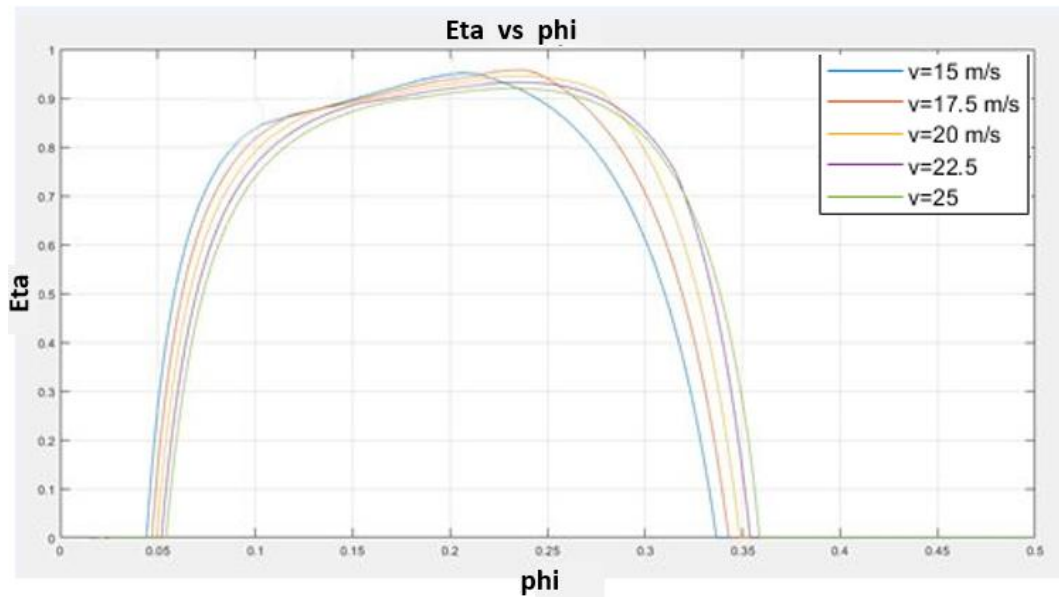
Fig. 2-17:efficiency as a function of phi

Predicted efficiencies are very high; this is due to the fact that the 1D model works as if there were no interferences between the blades. Intuitively the interaction between blades, and specifically acceleration between them should lead to higher pressure drops than the one predicted by 1D model, and finally lead to lower efficiencies.

EFFECT OF THE CHORD LENGTH:

A higher chord length has different effects:

- an increase of the pressure drop, as seen in (2.11)

- an effect on the power extracted, not only because of the chord length is directly appearing in (2.7) but also because of the modification of the Reynolds number.

-effect on kinetic energy of the wake, as a' in equation (2.10).is proportional to solidity, and so, to chord.

In (fig 2-19) the effects of different chord lengths are calculated for different tangential velocities making use of 1D calculations:
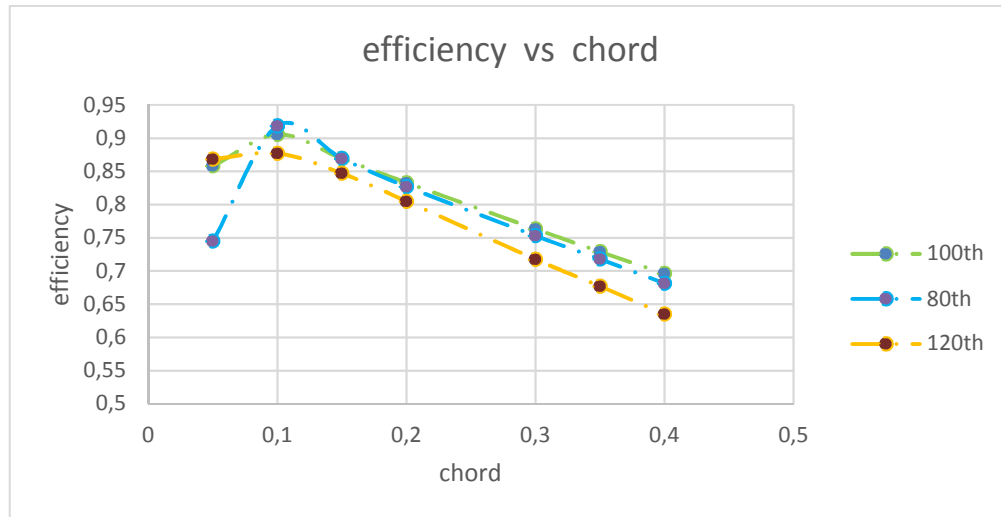
Fig. 2-18: efficiency as a function of chord length for different u velocities

It can be seen that Reynolds number effects determine one chord length which the optimal one in terms of efficiency.

EFFECT OF THE NUMBER OF BLADES:

The effect of number of blades according to this model is to :

-increase linearly the power extracted.

-increase linearly the static pressure drop

-increase linearly the rotational kinetic energy at the outlet

Since the pressure drop induced by the wake is subtracted to the static pressure drop, higher numbers of blades are expected to give higher efficiencies! In reality, the number of blades strongly affect the fluid region around the blades and so lift and drag coefficients, consistently power extracted and pressure drop do not grow linearly, because lift and drag coefficients are also changing with the number of blades. The 1D model is not able to predict what happens if number of blades is changed.

2.4   OPTIMIZATION:

To choose which combination of blade velocity, number of blades and chord length is the best choice , the Matlab code is not only structured to perform one calculation at a time but it is doing power and efficiency calculations given a specified ϕ and σ, which are identifying a geometry and first building a matrix in which the pressure drop is stored for all of these solutions:
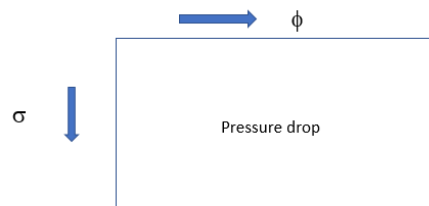
Having built the matrix, the code eliminates the solutions which don't satisfy the constraint on pressure drop, and build a similar efficiency matrix this time just with the efficiencies for acceptable solutions previously found.
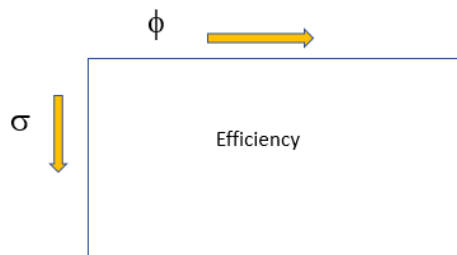
Actually σ depends on both chord and number of blades which of course are both unknown at the beginning, so not only σ is specified , but a number of blades is specified. Actually the scheme is the following (fig 2.20) in which only some number of blades are represented:
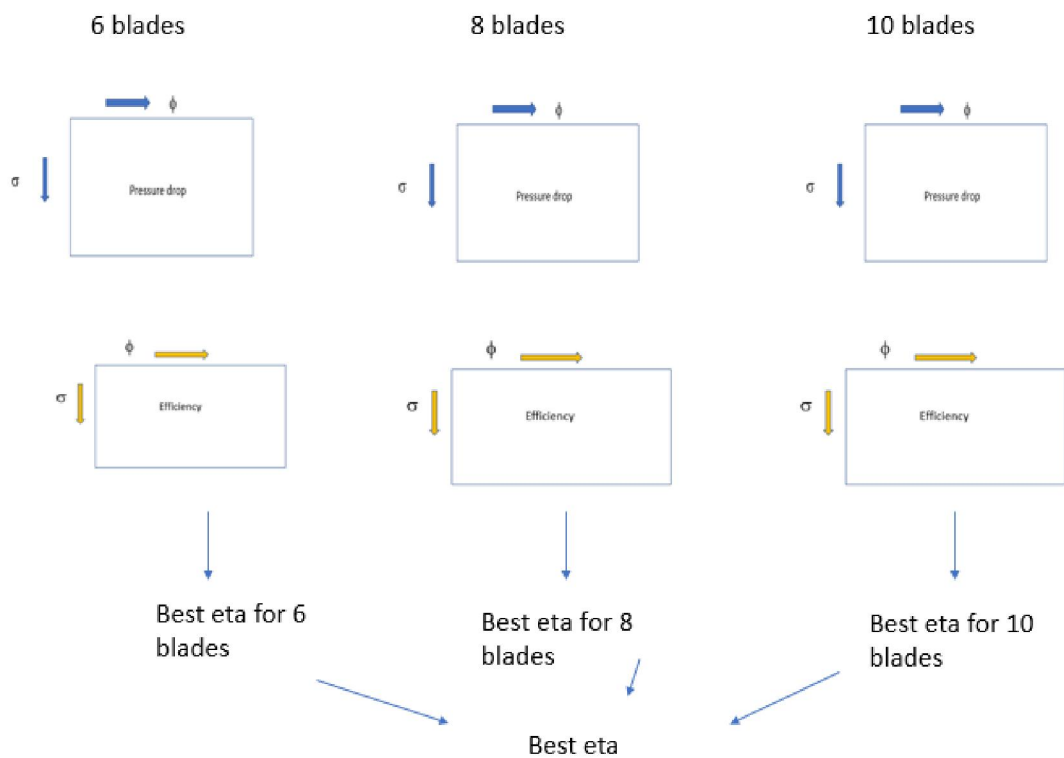
Fig. 2-19: scheme of the 1D matlab optimization code

The best solution for a particular number of blades is the one for which efficiency in the matrix is maximum. Then solutions of different matrices are compared, and the best one is found, so that finally also a number of blades can be chosen.

The results of this calculation are given in (fig. 2.21):

φ	0.16	0.17	0.2	0.22	0.23	0.25	0.23	0.22	0.18
u [m/s]	125	117.6	100	90.9	86.9	80	86.9	90.9	111
w [m/s]	126.6	119.3	102	93.1	89.2	82.5	89.2	93.1	112.9
alpha [°]	9	9.6	11.3	12.4	12.95	12	12.95	12.4	10.2
blades	2	4	6	8	10	12	14	16	18
chord [m]	0.235	0.13	0.11	0.095	0.085	0.08	0.065	0.055	0.035
Power [kW]	35,1	40,7	43,6	44,6	47,5	44,6	43,5	42,2	40,3
delta p [Pa]	952	972	1005	1000	1049	1031	1044	1041	1011
Efficiency	0.78	0.89	0.92	0.94	0.96	0.92	0.88	0.86	0.84

Fig. 2-20: optimal solutions of 1D matlab calculations

33

According to the 1D calculations the best solution is with 10 number of blades , and it's reported in (fig. 2.22)

φ	0.23
u [m/s]	86.9
w [m/s]	89.2
alpha [°]	12.95
blades	10
chord [m]	0.085
Power [kW]	47.4
delta p [Pa]	1049
efficiency	0.959
solidity	0.18

Fig. 2-21: best solution according to 1D Matlab model

But acceptable solutions that could reveal better after following 2D calculations could be with 6, 8, 12 number of blades. The chord lengths are around the values of 0.08-0.11 m.

Analysing the results it can be seen that all solutions lie in a range of solidity of [0.1- 0.2], (fig.2.23).

solidity	0.10	0.11	0.14	0.16	0.18	0.20	0.19	0.19	0.13

Fig. 2-22:range of solidities for the previous solutions

Solution with few blades must have a higher chord length to keep solidity in the range 0.1/0.15. These are not efficient solutions, since it was seen that higher chords decrease efficiency. Solution with higher number of blades must have lower values of chord length, but are also not practicable since the blades would be too thin!

2.5   2D DESIGN:

To develop a more precise analysis, a 2D model that takes into account tangential pressure and velocity distribution around the blade is developed using CFD software Star CCM+.

The code calculates the velocity and pressure distribution of the cascade, solving the following equations:

- Continuity equation
- Reynolds averaged Navier-Stokes equations
- Energy equation
- Turbulent kinetic energy equation
- Turbulent dissipation rate equation
- Substance state equation (ideal gas)

The turbulence model chosen is k-ϵ.

Since it is seen that to work far from stall the turbine has to be operated with high tangential velocity (around 100 m/s), compressibility effects are expected and so the energy equation has to be solved, together with ideal gas law, to calculate density variations.

To make the simulations, the geometric domain has been chosen as in (fig.2.24).
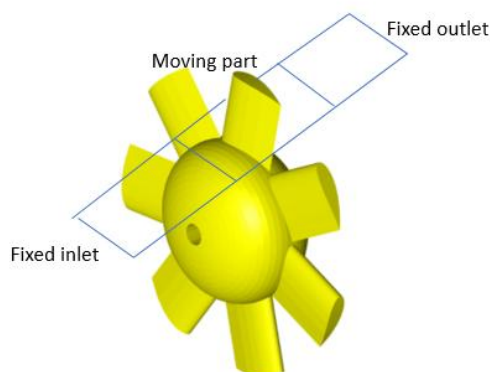
Due to the periodic condition of the fow between the blades, only one zone around the blade has been modelled with upstream and downstream zone. A frozen rotor

calculation has been used; this implies dividing the domain in three regions, a fixed zone upstream and downstream, and a central zone which takes into account the effects of rotation, but without really moving (it takes into account the forces of inertia).

 A mesh with a total number of cells of about 47000 has been built (fig.2.24). It consists of two fixed parts and a central moving one on which a translation equal to blade velocity is imposed. A zoomed view of the mesh around the blade is given in (fig. 2.23). The inlet region is modelled with a velocity inlet boundary condition imposing an axial velocity of 20 m/s; the outlet is modelled with an outlet pressure boundary condition imposing a relative pressure equal to 0. The sides of the three regions are modelled with a periodic boundary condition.
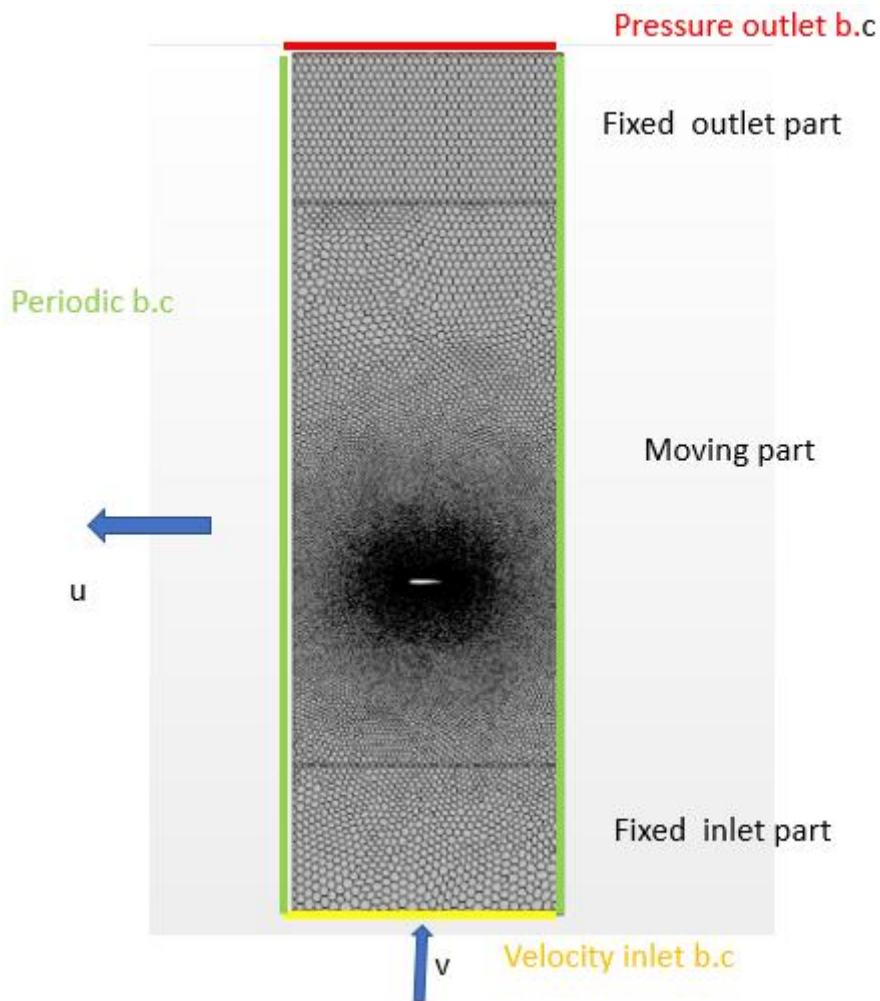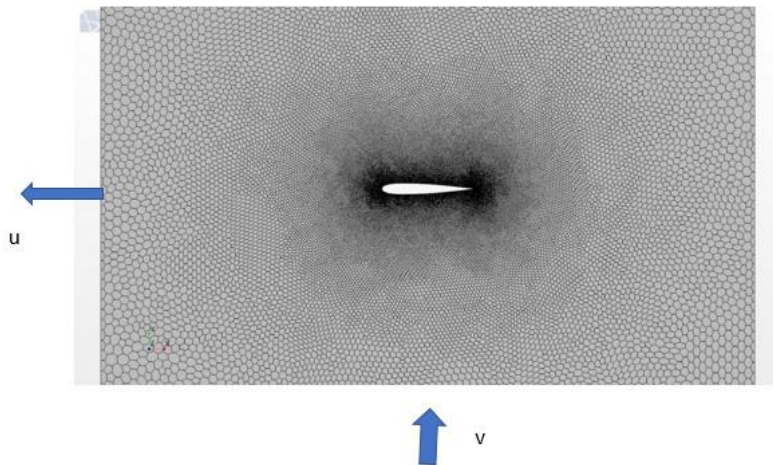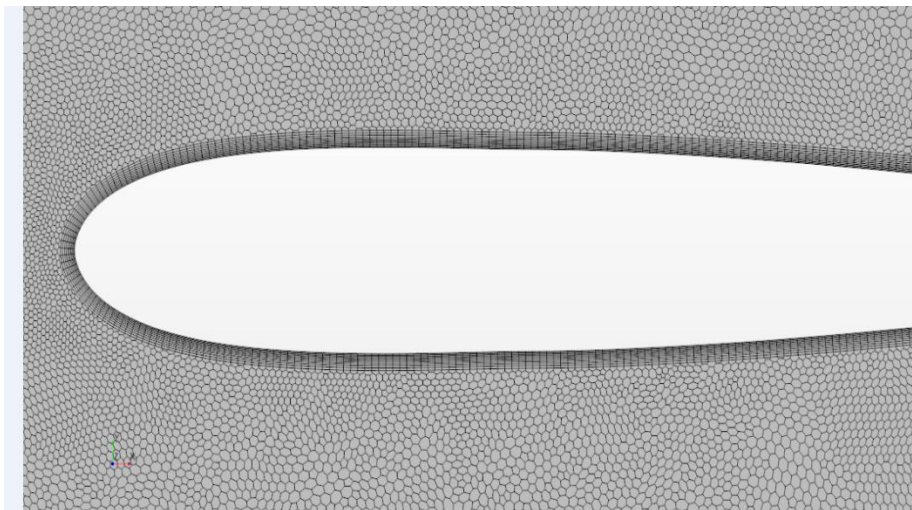

Fig. 2-23: 2D mesh for Wells turbine

Fig. 2-24: zoom of the 2D mesh around the blade

Simulations have been made for the particular case of v= 20 m/s and 8 blades , which is usually the number of blades used in many applications [9] and was one of the possible choices according to 1D model, but different values of chord lengths have been tested for various u velocities in order to make a comparison between forces F, thrust and pressure drop calculated with the 1 D model and the 2D model. It has been found that:

-As far as tangential forces are concerned 1D calculations are underestimating their values, except for low values of chord length. This has to be attributed to the mutual interference effect that was mentioned before.

-pressure drop increases almost linearly with blade velocity and in exact proportion with axial force as predicted by momentum theory. It was also found that the increase is more than linear with chord length, following $\Delta p \propto \sigma^{1.6}$ as reported in [11].

- kinetic energy in the wake increases with blade velocity and chord length

The detailed description of results for pressure drops and forces is found in appendix B. In the following, only results for power coefficient curves (fig.2.26), (fig.2.27) and efficiency curves (fig.2.28) are reported;
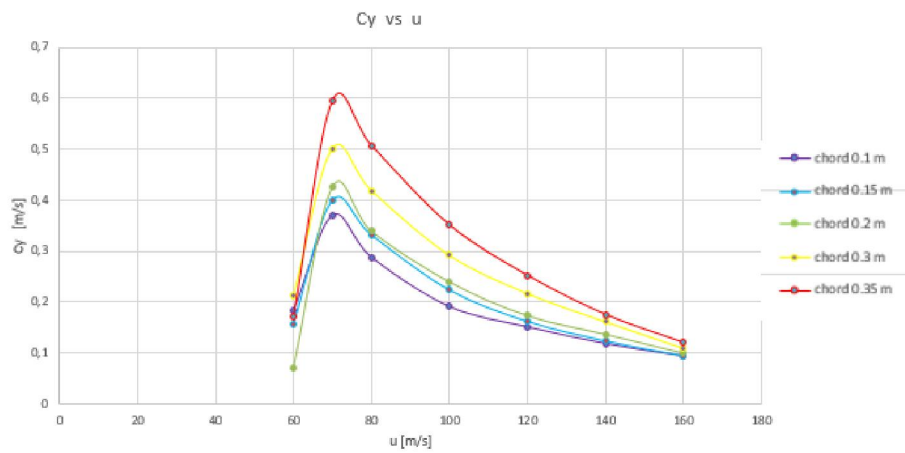

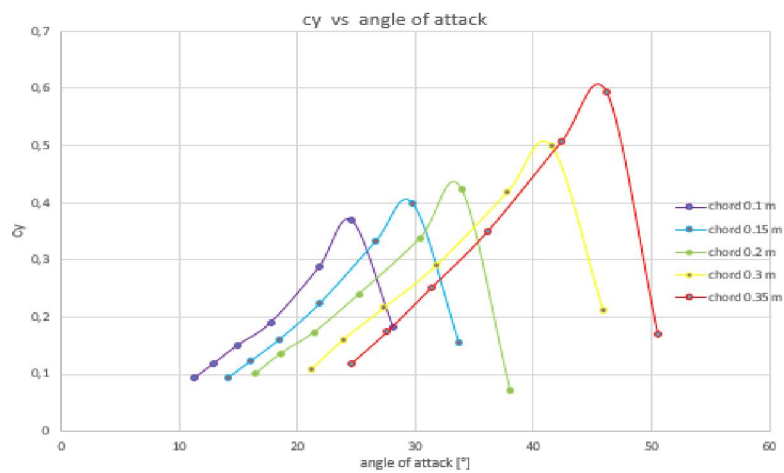*Fig. 2-25: cy coefficient as a function of u velocity*

Fig. 2-26: cy coefficient as a function of angle of attack

The effect of bigger chord lengths on power coefficient is to increase it: the interference effect on velocity triangles shape allows to have maximum lift at a higher angle of attacks (fig.2.27) so that it is said that solidity sustain lift, as it is reported in many articles [11].

The efficiency curve as a function of u velocity for different chord lengths is shown in (fig.2.28).
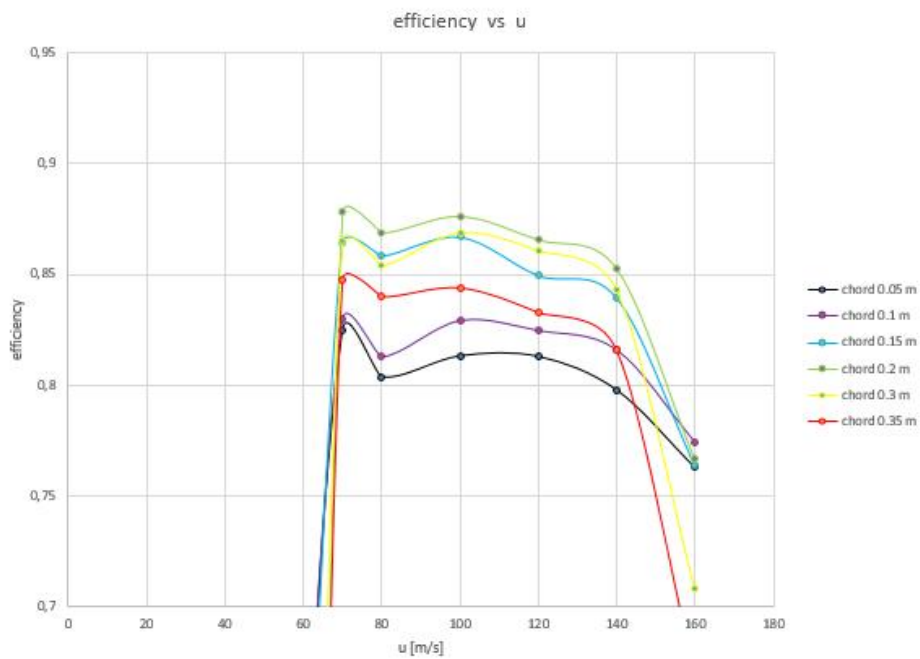

Fig. 2-27: efficiency as a function of u velocity

In (fig.2.29), efficiency is plotted as a function of phi, showing also the differences with 1D predicted efficiencies:
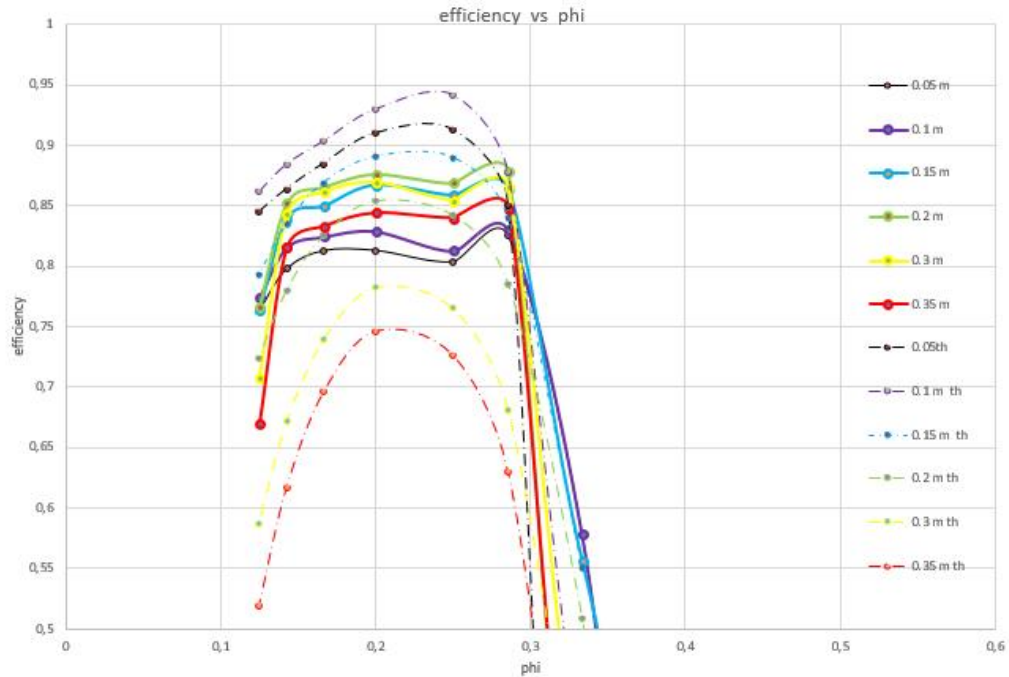
Fig. 2-28: efficiency as a function of phi for 1D model (dashed lines) and 2D model (continuous lines)

1D model underestimates performance for chord lengths of 0.35 and 0.3 m but overestimates performance for chord lengths lower than 0.2 m.

The difference between 1D and 2D models is due to the following reasons:

$$\frac{\eta_{2D}}{\eta_{1D}} = \frac{(\frac{F}{\Delta p_0})_{2D}}{(\frac{F}{\Delta p_0})_{1D}}$$

The fact that as a general rule efficiency of 2D model is lower is caused by a lower $\frac{F}{\Delta p_0}$ ratio, since 2D model estimates higher pressure losses caused by friction that 1D model cannot catch and due the different deflection evaluated due the interference effect..

The fact that predicted efficiency of 2D model is higher than 1D for chord length of 0.3 m and 0.35 is related to the wake downstream of the turbine: the more kinetic energy contained in the wake, the less the total pressure drop, with the result that

40

high chord lengths are less penalized than what 1D model would predict since 1D model underestimates the energy in the wake.

The shapes of the curves give a hint on how to choose rotational velocity: a good choice for u velocity could be 100 m/s since is mid way from stalling region that should be avoided in most operating conditions as possible, and to drag region in which low angle of attack brings down efficiency. Lower velocities as 80 m/s are next to the maximum before stall, and even if more efficient points, a rotational velocity variation can lead more easily to stall.

The design blade velocity is chosen to be 100 m/s, corresponding to 1275 rpm.

EFFECT OF CHORD LENGTH:

As for the 1D case, the curves of efficiency as a function of chord length for 8 blades are plotted in (fig.2.30):
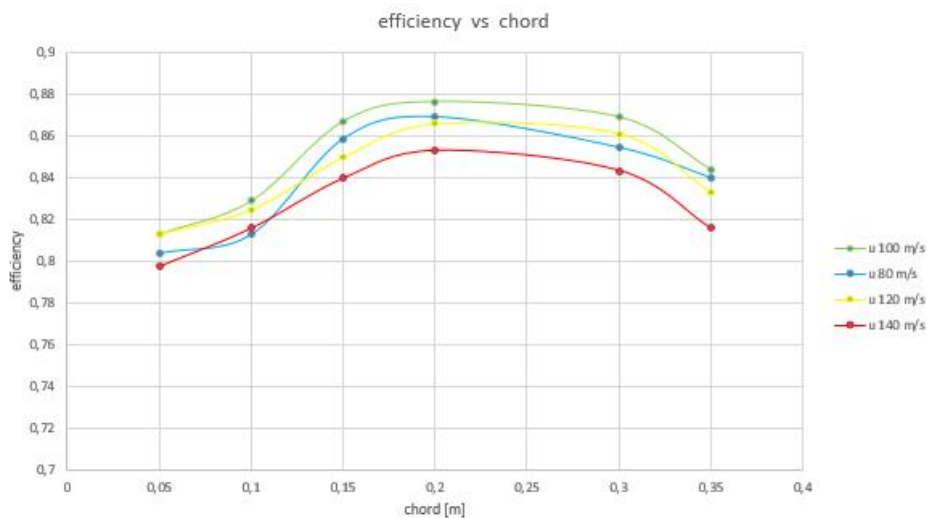

Fig. 2-29: efficiencies as function of chord length for different u velocities

As for the 1D calculations, also in 2D there is a maximum of the curve; the maximum predicted by 1D calculations was for chord length 0.1 m, and in 2D calculations the maximum is shifted towards 0.17 or 0.2 m. The effect of solidity seems to privilege higher values of chord.

EFFECT OF NUMBER OF BLADES:

Efficiency and power curves have been investigated for a turbine with 8 number of blades; what has been done is to investigate also the effect of 4, 6, or 10 number of blades to optimize the turbine .

The number of blades has an effect on solidity; intuitively the effect should be similar of the one caused by a longer or shorter chord. But changing the chord has an important effect on the boundary layer of the blade, and so to lift and drag coefficients.

A blade velocity of 100 m/s is chosen, and different configurations with different solidities were tested (fig.2.31):

Chord [m]

solidity	0.10	0.15	0.20	0.30
4	0.08	0.13	0.17	0.25
6	0.13	0.19	0.25	0.38
8	0.17	0.25	0.34	0.51
10	0.21	0.32	0.42	0.64

Blades

Fig. 2-30: various solidities tested in 2D calculations

For these solidities, total pressure drops are reported in (fig.2.32):

Chord [m]

Delta_p_tot [Pa]	0.1	0.15	0.2	0.3
4	562	928	1276	2052
6	883	1433	2000	3390
8	1350	2006	2791	5235
10	1520	2627	3899	7542

Blades

Fig. 2-31:total pressure drops for the tested cases

The total pressure drop increases with solidity, as expected (fig.2.33). The increase is more than linear , as already underlined.
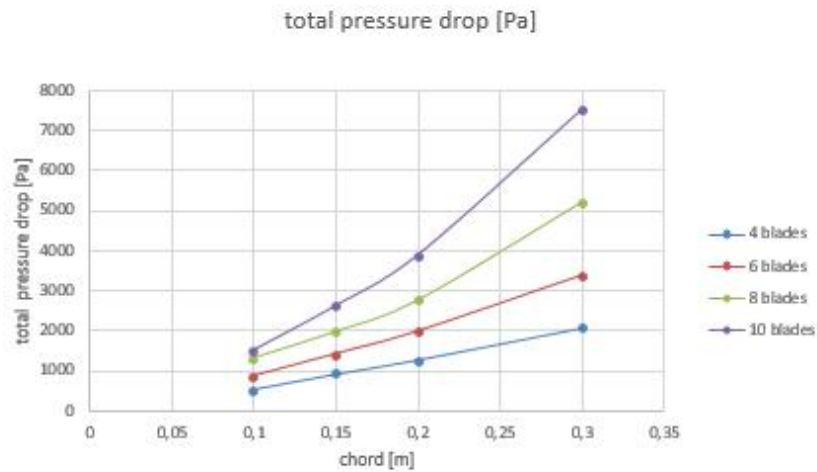
Fig. 2-32: total pressure drops of figure 1.53 expressed as a function of chord

Since the design must be done with a constraint on pressure drop, only solutions with low solidity, as the ones the Matlab 1D program was choosing are possible. Actually it is seen that 8 and 10 blades are giving higher pressure losses if not for low values of chord length, possibly lower than 0.1 m. But as the efficiency plot (fig.2.34 and fig.2.35) shows, that these are not corresponding to good efficiencies:

		Chord [m]		
efficiency	0.1	0.15	0.2	0.3
4	0.786	0.860	0.869	0.863
6	0.815	0.862	0.870	0.857
8	0.830	0.868	0.876	0.868
10	0.810	0.869	0.874	0.866

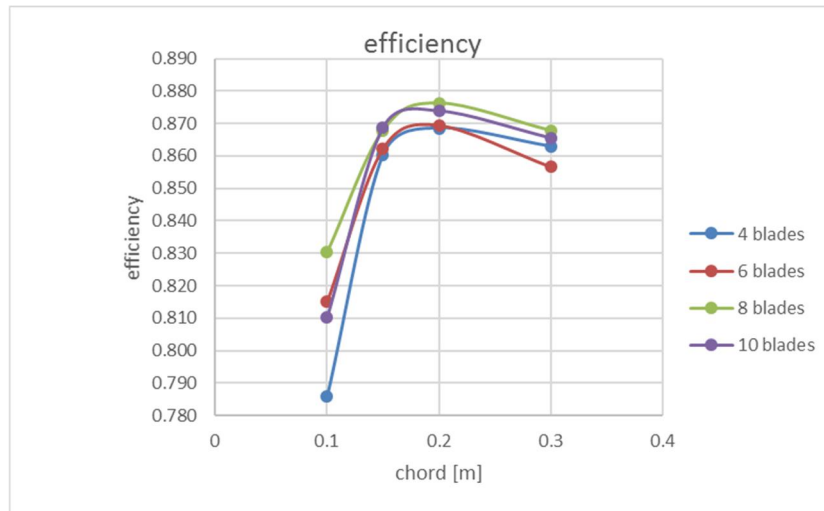*Fig. 2-33: efficiencies for the tested solutions*

Fig. 2-34: efficiencies of figure 1.55 expressed as a function of chord

Due to the results plotted in figure (fig 2.35) some more simulations have been done for 4 blades. The best solution proposed for Wells turbine is reported in (fig. 2.37)

blades	4
chord [m]	0.165
Fx [N]	105.5
delta p tot [Pa]	1029
delta p static [Pa]	1065
power [kW]	42
Q [m^3/s]	23.55
eta	0.871

Fig. 2-35: best solution according to 2D calculations

In the design conditions, CFD simulations give the following velocity and pressure distributions around the blade, reported in figures (fig 2.38), (fig.2.39) and (fig.2.40);
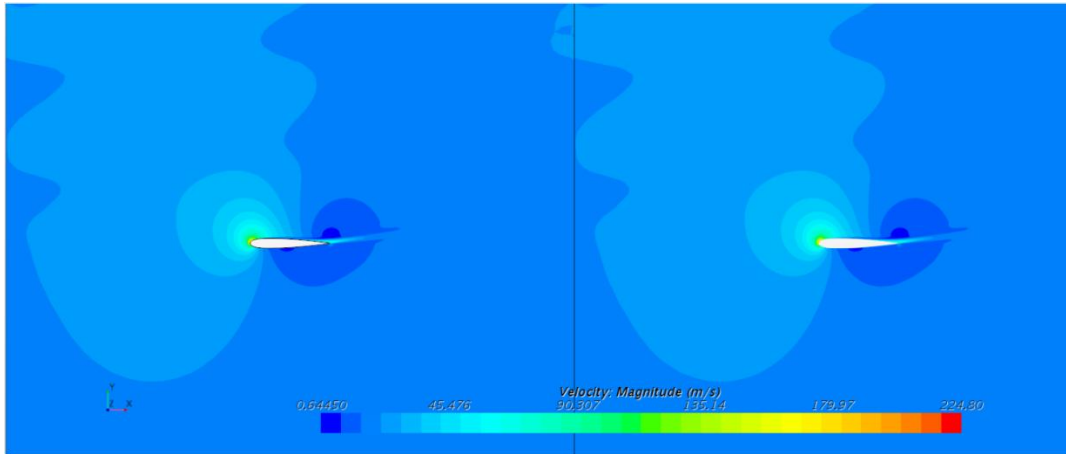
44

Fig. 2-36: absolute velocity magnitude scene

Interaction between neighbouring blades is reduced, and in fact 1D and 2D calculations were giving similar results for chord lengths of 0.15 m or 0.2m (fig.2.29).
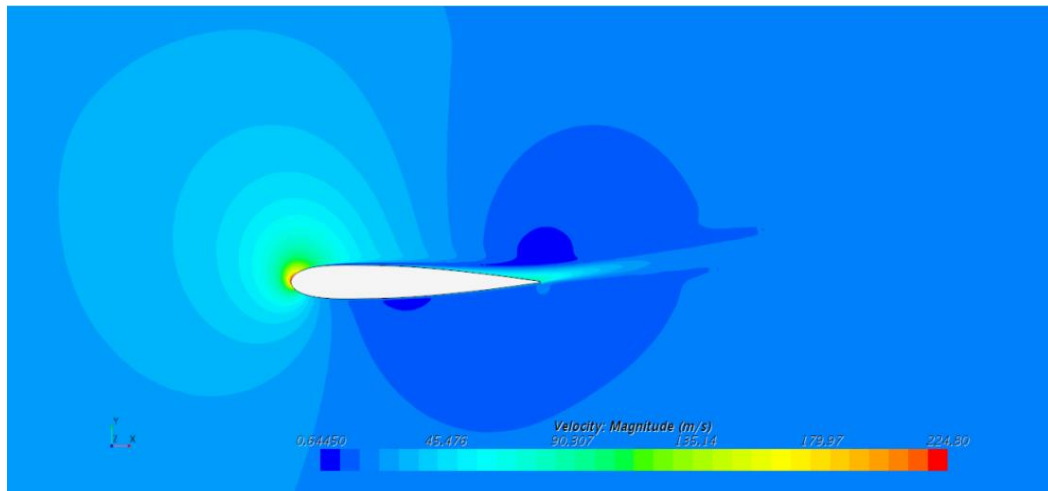

Fig. 2-37: absolute velocity magnitude scene for only one of the blades

At the leading edge (fig.2.39) a strong acceleration is present, giving a local velocity of 224 m/s, which justifies the use of a compressible flow model in CFD calculations.
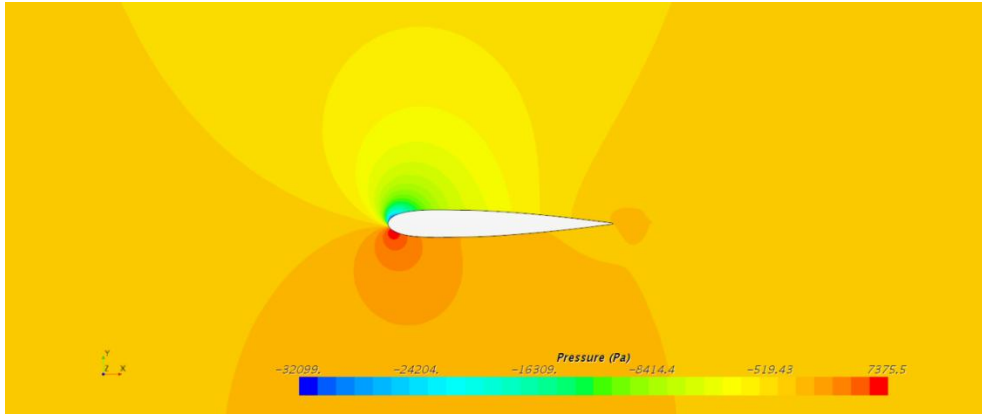
Fig. 2-38: static pressure scene

From relative velocity vector plot (fig.2.41) it is possible to see the incoming flow with it's angle of attack of

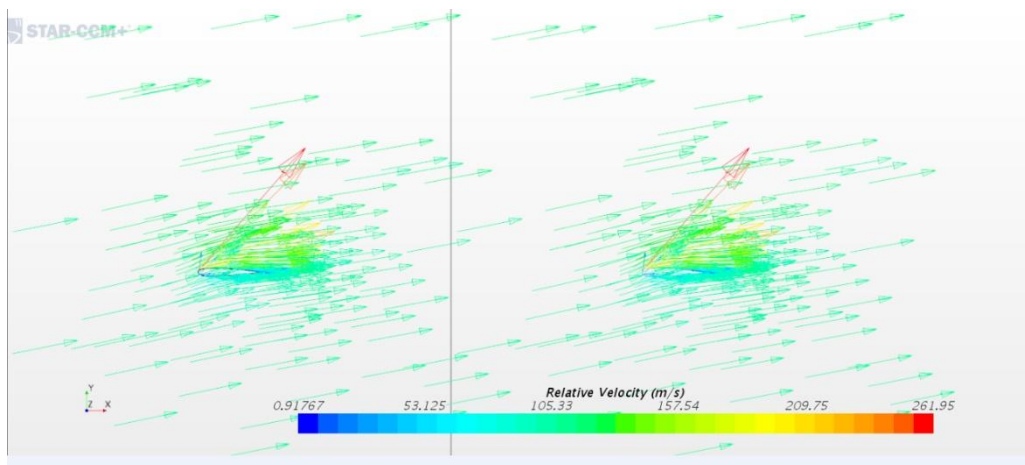$$\alpha = arctan\frac{20}{100} = 11.3°$$

Fig. 2-39: relative velocity vector scene

The absolute velocity vector plot (fig 2.42), shows the wake rotation with the turning of the flow after the plane of rotation, and the acquisition of a tangential component of velocity.
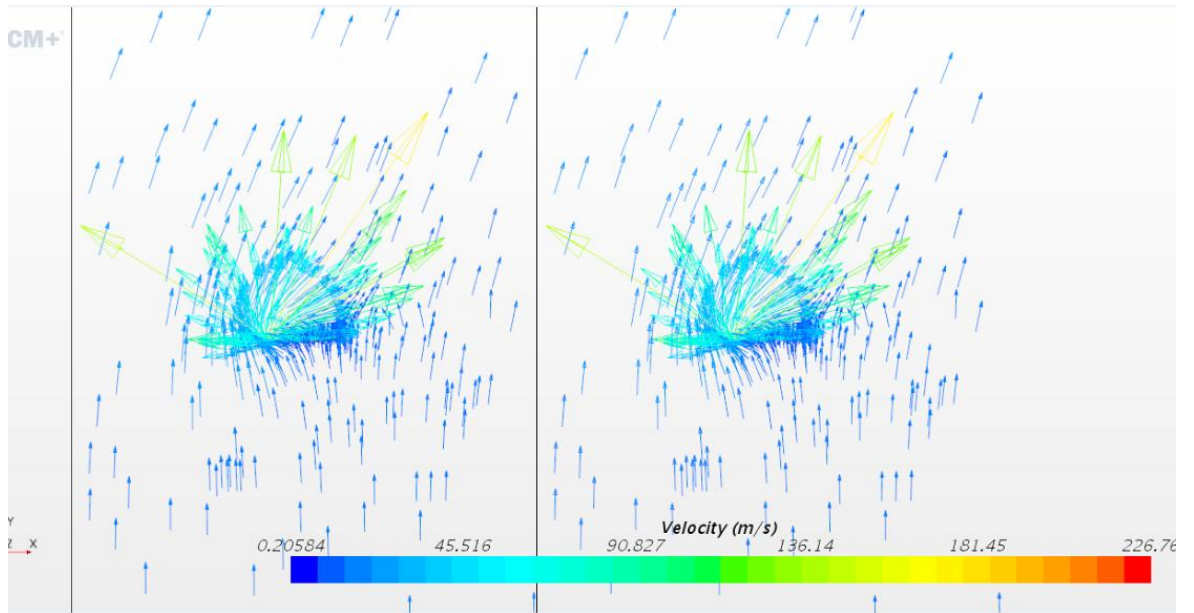
46

Fig. 2-40:absolute velocity vector scene

The vorticity in the wake of the turbine is represented in the following figure (2.43):
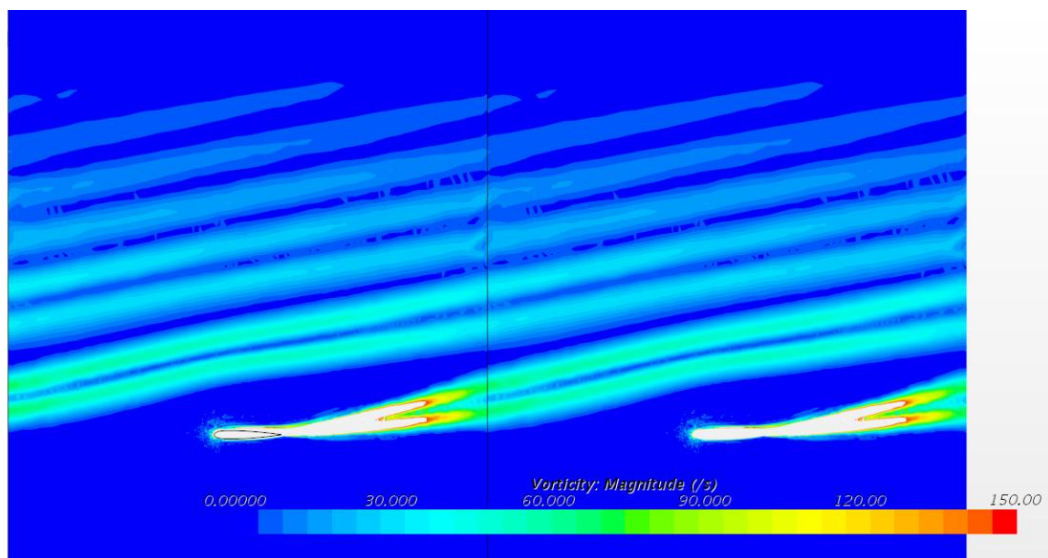

Fig. 2-41: vorticity magnitude vector scene

2.6   OFF   DESIGN   PRFORMANCE:

Since during operation the turbine has to face different wind conditions than the 20 m/s design one, the steady state behaviour of the machine chosen as the best solution (fig.2.37) has been tested for different air flow velocities: different

simulations have been done for a tangential velocity u of 100 m/s with a different air flow absolute velocity: power and efficiency curves for different air flow velocities are represented in (fig.2.44) and (fi.2.45).
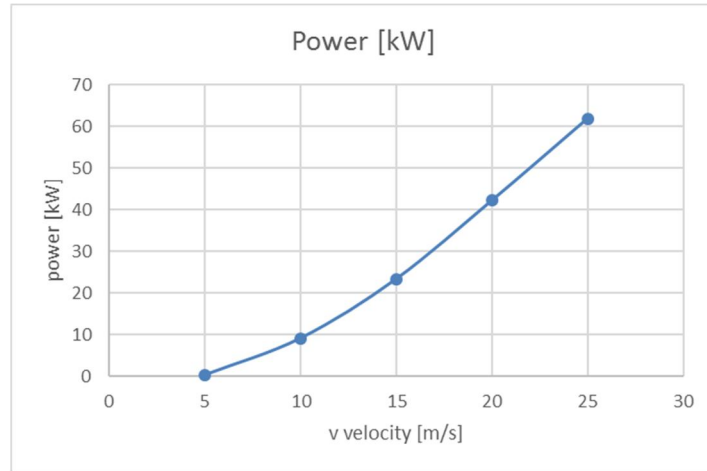

Fig. 2-42 estimated power production for the chosen turbine as a function of air flow velocity
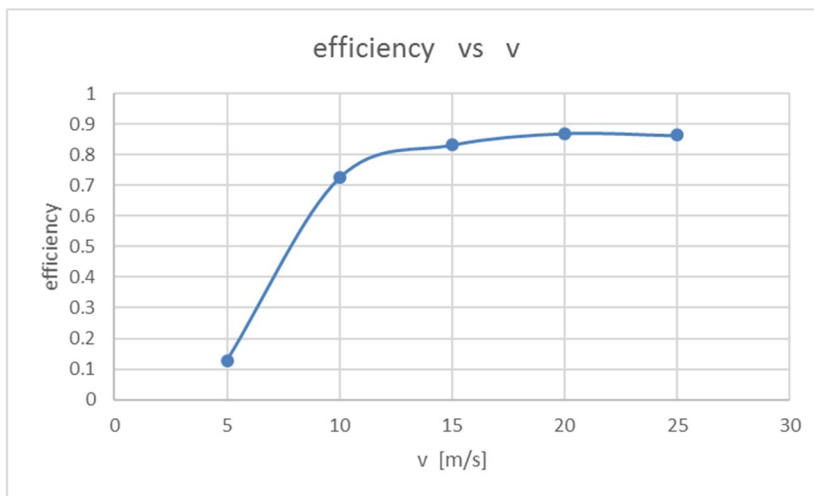

Fig. 2-43:efficiency for the chosen turbine as a function of air flow velocity

In this chapter, a design of the Wells turbine has been proposed after having built a 1D code, and a 2D model to validate 1D model and investigate with more precision which solution is the best one.

In the next chapter the same procedure is followed for Impulse turbine, aiming to find at the end of next chapter the best design solution for Impulse turbine.

3 IMPULSE TURBINE:

In this chapter a design for Impulse turbine is proposed: first, a description of the main peculiarities related to the symmetry constraint of the turbine is given, and a simple analytical model based on Euler's equation is used, then a code in Matlab is developed based on pressure drop correlations to optimize the geometry of the turbine. A 2D model is ultimately developed in Star-CCM+ to validate 1D results.
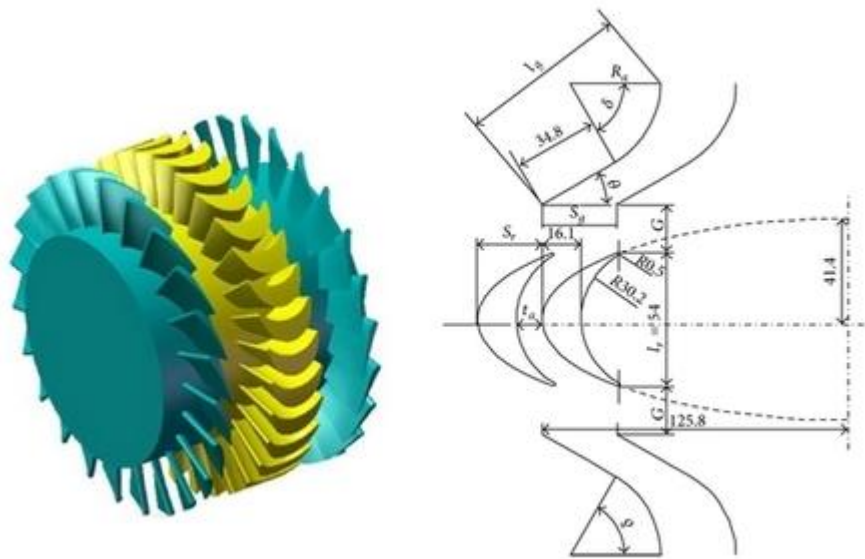

Fig. 3-1:geometry of Impulse turbine; taken from[www.scoop.it/turbines/p/4007344956/2013/09/09/numerical-analysis-of-impulse-turbine-for-isolated-pilot-owc-system]

Self-rectifying Impulse turbine consist of 3 rows of blades, in particular one rotor and two stators (fig.3.1) and it is thought for OWC plants [12].

As for Wells turbine the machine is represented in a plane section and using triangles of velocity (fig.3.2):
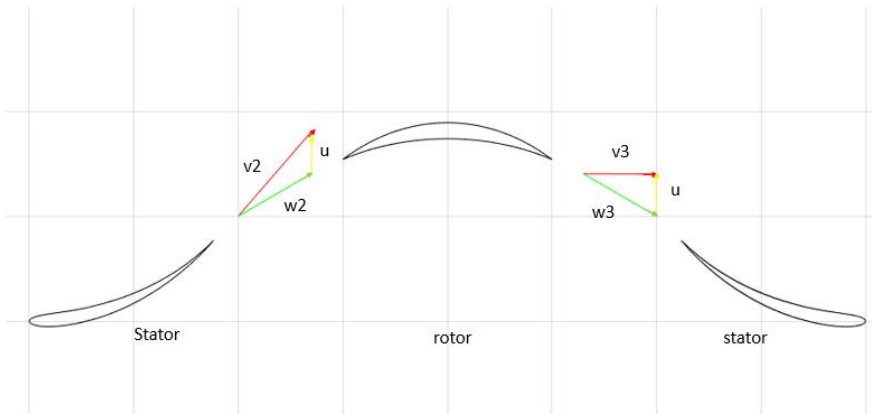
Fig. 3-2:velocity triangles for impulse turbine

The one shown in (fig.3.2) is a different configuration than the usual impulse turbine for which one stage corresponds to a stator row, followed by a rotor (fig.3.3). The usual configuration in (fig 3.3) is used in steam turbines, but in the case of 3 row self-rectifying, the difference is due to a symmetry constraint.
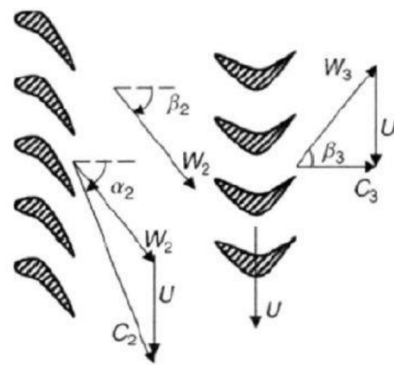

Fig. 3-3 typical impulse stage for a steam turbine; taken from [F

3.1 SIMMETRY CONSTRAINT

In order to work as a self-rectifying turbine, the inlet and the exit flow of the machine have to be both axial, because what is exit in one sense, becomes entry in the other! If the flow is reversed, the relative velocity w1 should be like in figure (fig 3.4) to make the rotor turning, but it is an unrealistic situation since the big

50

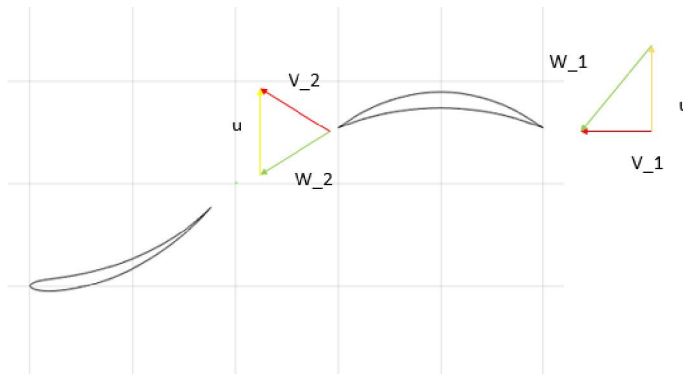difference between flow angle and blade angle could not allow sufficient torque to be developed.

Fig. 3-4 triangles of velocity that would be required if the flow is reversed for one stator,one rotor

The possible solution of the problem is to use another stator row to guide the flow into the rotor if the flow is reversed, as in figure (fig.3.5)

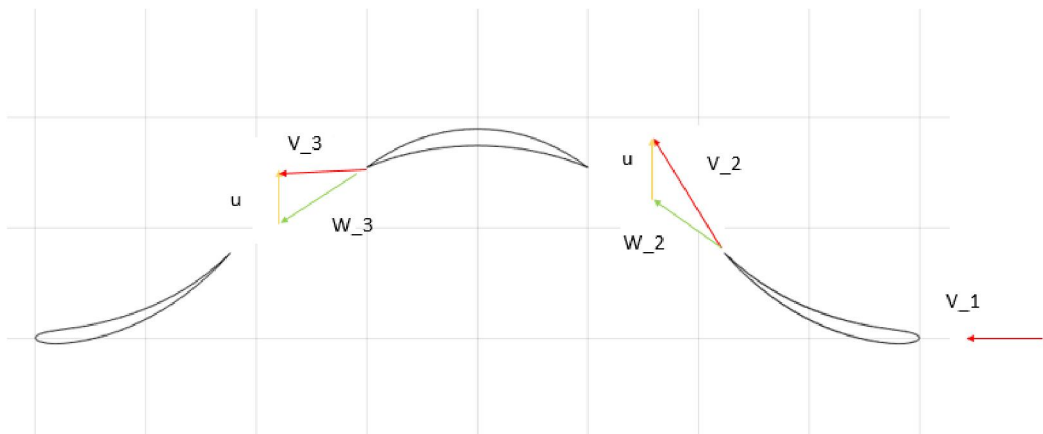Fig. 3-5 triangles of velocity when the flow is reversed

Looking at both figures (fig.3.2) and (fig 3.5), however, it is clear that one problem persists: using a second stator row implies that the entrance to the second stator is different from the optimal one in which flow angle is equal to blade angle. This causes shock losses at the inlet of the second stator. Figure (fig 3.6) is a reference for the angles.
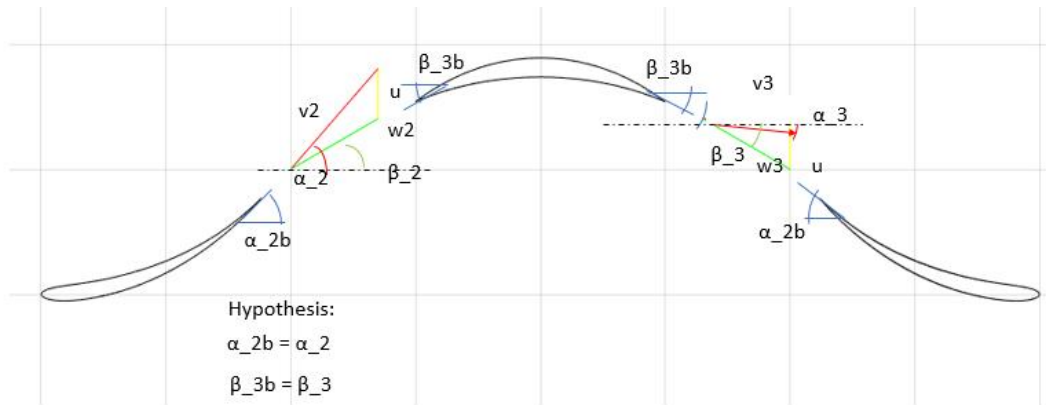
Fig. 3-6a velocity and angles for impulse turbine

Looking at (fig.3.6a) it is possible to reduce shock losses at the second stator deliberately choosing the rotor blade inlet angle (β_{2b}) to be higher than the flow angle (fig.6.b). This will introduce some shock losses at the rotor inlet, but at the same time the shock losses at the second stator will be reduced, because angle α_3 will increase. It is possible that the shock losses in the second situation (fig.6.b) are lower than in the case in figure(3.6a).
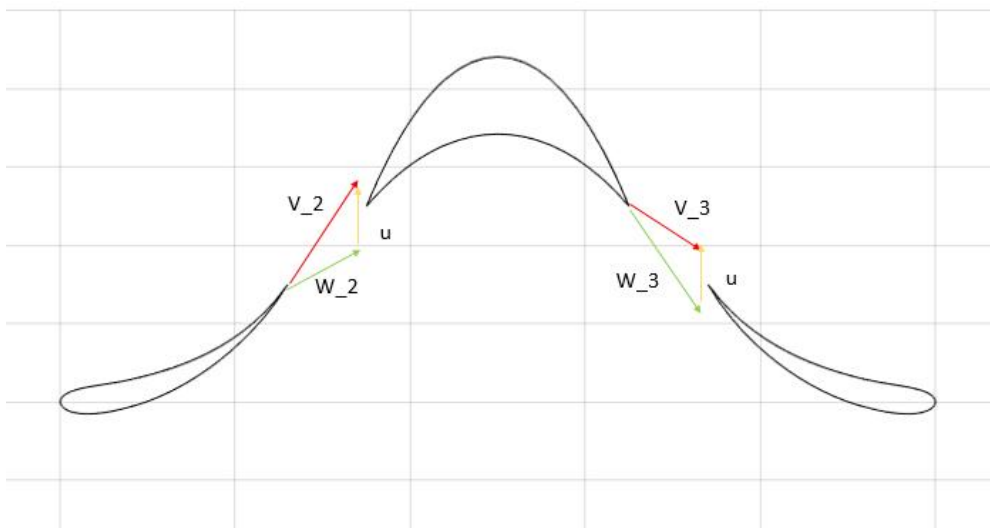

Figure 3.6b:velocity triagles in the case of shock losses present at both rotor and stator

 To design the turbine in the best way, it is necessary to estimate which combination of the angles α_{b2} and β_{b2} determine the lowest shock losses.

3.2 EULER EQUATION

Using basic physics knowledge, power extracted by the turbine can be calculated by law of angular momentum applied to the central rotor, as was done also for Wells turbine:

$$P = \omega * T = \dot{m} * \omega * r * (v_{t2} - v_{t3}) \tag{3.1}$$

Power produced by the turbine is torque times the angular velocity, and torque is equal to the change of moment of momentum, which implies tangential components of absolute velocities (in blue in figure fig.3.7): bigger this difference, bigger the power extracted.
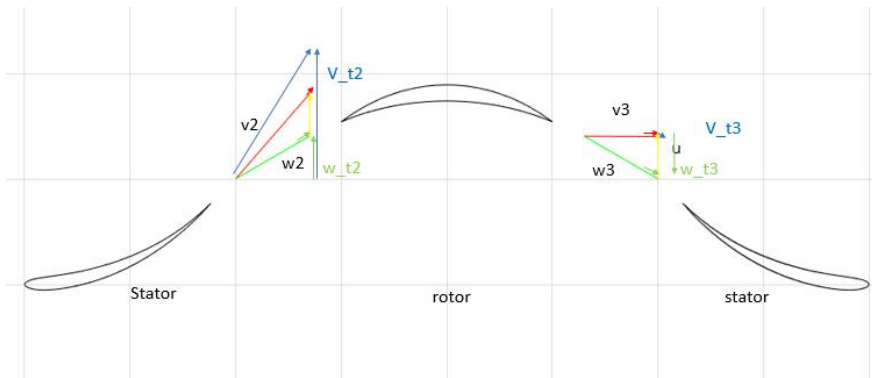

Fig. 3-7 tangential components of velocity

Substituting for mass flow rate in (3.1):

$$P = \rho \cdot A \cdot v \cdot u \cdot (v_{t2} - v_{t3})$$

By considering velocity triangles (fig.3.2), the following holds:

$$P = \rho \cdot A \cdot v \cdot u \cdot (w_{t2} + u + w_{t3} - u)$$

$$P = \rho \cdot A \cdot v \cdot u \cdot (w_{t2} + w_{t3})$$

$$P = \rho \cdot A \cdot v \cdot u \cdot v \cdot (\tan \beta_2 + \tan \beta_3)$$

To express velocity in terms of the blade angles and $\phi = \frac{v}{u}$, two expressions derived using trigonometry on triangles of velocity are used:

$$\begin{cases} \tan \alpha_2 - \tan \beta_2 = \dfrac{1}{\phi} \\ \tan \beta_3 - \tan \alpha_3 = \dfrac{1}{\phi} \end{cases} \tag{3.2}$$

By substituting (3.2) in (3.1), power becomes:

$$P = \rho \cdot A \cdot v^2 \cdot u \cdot (\tan \alpha_2 - \frac{1}{\phi} + \tan \beta_3)$$

$$P = \rho \cdot A \cdot \frac{v^3}{\phi} \cdot (\tan \alpha_2 - \frac{1}{\phi} + \tan \beta_3) \tag{6.3}$$

The coefficient

$$\frac{1}{\phi} \cdot (\tan \alpha_2 - \frac{1}{\phi} + \tan \beta_3) \tag{3.7}$$

can be plotted as a function of ϕ (fig.3.8): a value of 60° for both the angles is assumed ;
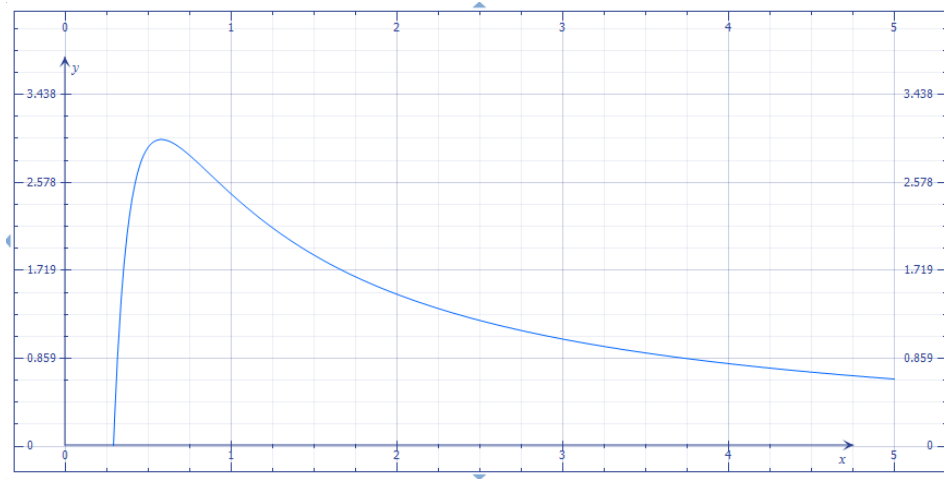
Fig. 3-8: power coefficient in (4) as a function of phi

According to Euler equation, there is a maximum value of the power that can be extracted given a velocity of the incoming air flow.

The tangential force is:

$$F = \rho \cdot A \cdot v^2 \cdot (\tan \alpha_2 - \frac{1}{\phi} + \tan \beta_3)$$

As for power, it is defined a coefficient :

$$(\tan \alpha_2 - \frac{1}{\phi} + \tan \beta_3) \qquad (3.8)$$

These coefficients are not defined in the same way as was done for Wells turbine but the comparison between the two turbines has not been based on dimensionless force and power coefficient, rather on efficiency and pressure drop.

If the force and power coefficients are plotted as a function of u velocity for a fixed v of 20 m/s, it can be seen that force decreases linearly with increasing rotational velocity and power reaches a maximum at around u=36 m/s ($\phi = 0.56$) as can be seen also in (fig.3.9)
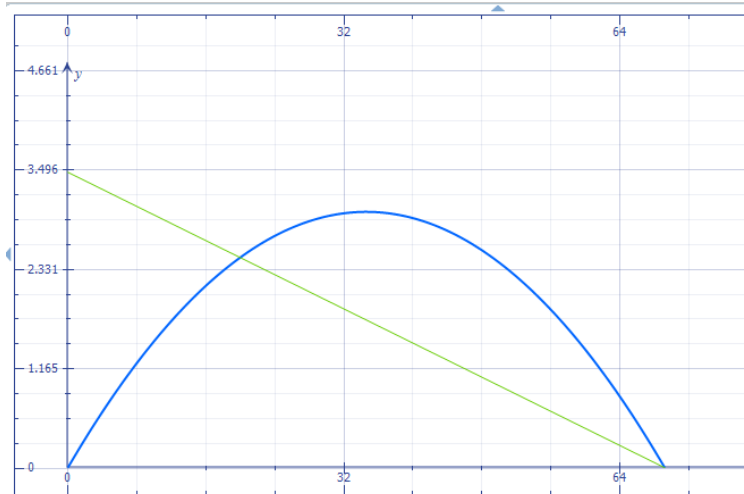
Fig. 3-9: force and power coefficients given in () and () as a function of u[m/s]

This is the classical shape of the curves for a traditional impulse turbine.

The next piece of information is efficiency, which depends on pressure drop; between inlet and outlet of the machine, the energy balance is:

$$\frac{p_4 - p_1}{\rho} + \frac{v_4^2 - v_1^2}{2} + \frac{\Delta p_{loss_{s1+r+s2}}}{\rho} = L$$

Where L is specific work [J/kg] corresponding to:

$$L = \frac{P}{\dot{m}}$$

If velocity at inlet and outlet are assumed to be equal, so that total pressure drop is equal to static pressure drop, efficiency becomes:

$$\eta = \frac{L}{\Delta p} = \frac{L}{L + \Delta p_{loss_{s1+r+s2}}} = \frac{1}{1 + \dfrac{\Delta p_{loss_{s1+r+s2}}}{L}} \qquad (3.6)$$

A very simple model to describe pressure losses is to consider them to be the ones concentrated at the inlet of the rotor and the stator due to the shock losses, which could be expressed as:

$$\Delta p_{loss_{s1+r+s2}} = k_r \cdot \frac{w_2^2}{2} + k_{s2} \cdot \frac{v_3^2}{2}$$

Assuming the loss coefficients as equal to each other,

$$\Delta p_{loss_{s1+r+s2}} = k\left(\frac{v_3^2}{2} + \frac{w_2^2}{2}\right) \qquad (3.7)$$

To look for the maximum efficiency from (3.6), the quantity $\frac{\Delta p_{loss_{s1+r+s2}}}{L}$ has to be minimized; this can be done by expressing velocities in terms of the angles and phi (using 3.2) and setting the derivative with respect to phi equal to 0. If this is done it is found that:

$$\phi = \frac{2}{(\tan \alpha_2 + \tan \beta_3)} \qquad (3.8)$$

Using eqn.(3.8) it can be shown that optimal angle configuration should be:

$$\begin{cases} \alpha_2 = \beta_3 \\ \beta_2 = \alpha_3 \end{cases} \qquad (3.9)$$

This means that the velocity triangles are symmetric, as in the following (fig.3.10), and that the optimal configuration is the one in which shock losses are distributed equally at the rotor and at the second stator!
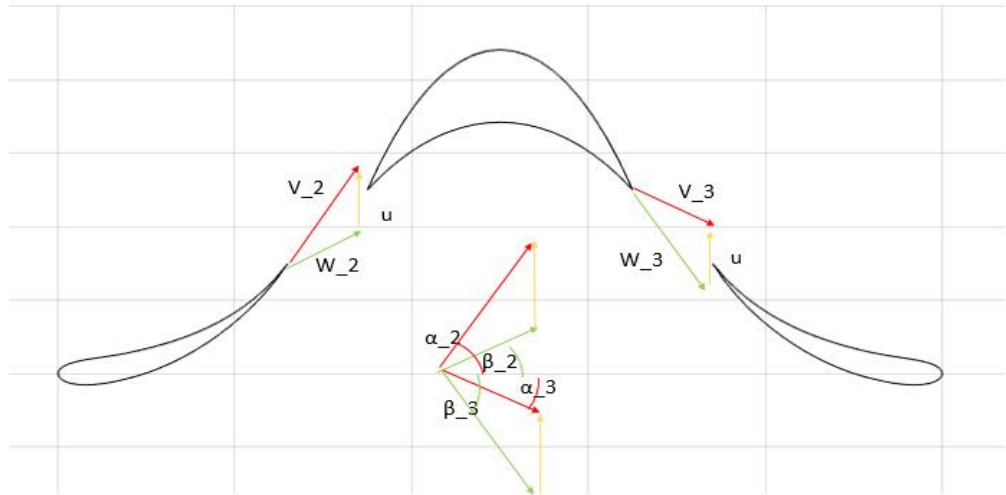
Fig. 3-10:optimal triangles of velocity

Actually, the loss coefficients are not constant with ϕ and they depend on the angles; to have a more precise model of the turbine, pressure loss coefficients have to be found as a function of the relevant parameters of the machine. These loss coefficients are calculated usually using correlations, semi-empirical equations based on experimental observations which usually permit to calculate pressure changes for each row in terms of angles of the blade, span to chord ratio, and other parameters [6], [4].

3.3 CORRELATIONS:

The correlations are expressed in terms of a pressure loss coefficient that permits to calculate the pressure drop for each stage; this coefficient is defined as:

$$c = \frac{\Delta p_{tot\_stage}}{\Delta p_{tot\_stage} - \Delta p_{static-stage}}$$

Two extensively used correlations used for turbines and compressors have been used to build a Matlab code to calculate the performance of the turbine and to optimize it:

-Ainley Mathieson

- Howell

In the following, the two correlations are briefly described, leaving more detailed explanation to references [6], [4].

AINLEY MATHIESON :

The correlation of Ainley Mathieson [4] was developed making experiments over a broad range of axial flow gas turbines and it is expressed in terms of a loss coefficient defined as:

$$Y = \frac{\text{Loss of total-head pressure}}{\text{Total pressure at blade outlet} - \text{static pressure at blade outlet}} \ .$$

The main parameters which are affecting pressure losses are incidence, defined as in figure (fig 3.11), Mach number, Reynolds number.

FIG. 2a. Gas angle notation.
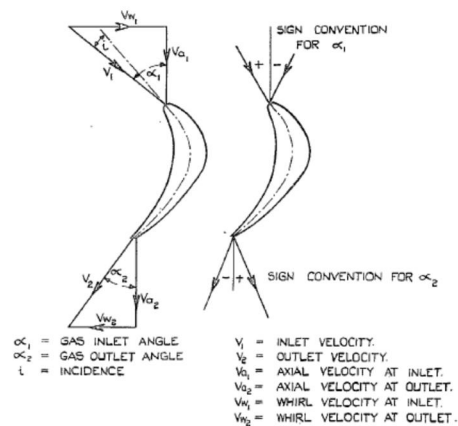
Fig. 3-11: angles definitions for Ainley Mathieson; taken from[4]

Experiments were done at zero incidence for nozzle blades and impulse blades, and two loss coefficient are expressed for these two types of blades as function of pitch to chord ratio and outlet gas angle. The values for loss coefficient are found in Ainley Mathieson and are reported in figures (fig.3.12) and (fig.3.13):
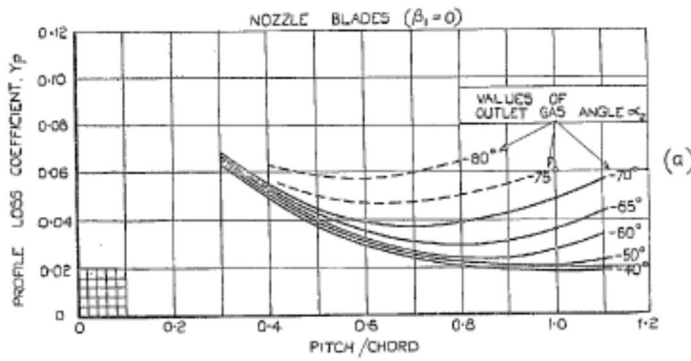
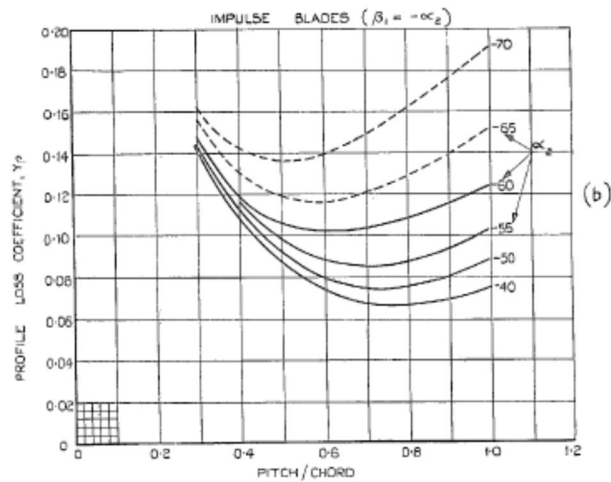Fig. 3-12:loss coefficient given by Ainley Mathieson; taken from[4]

FIG. 4. Profile-loss coefficients for conventional section blades at zero incidence. $t/c = 20$ per cent; $Re = 2 \times 10^5$; $M < 0.6$.

Fig. 3-13: loss coefficient given by Ainley Mathieson; taken from[4]

For conventional blades, intermediate between nozzle and impulse, the results are interpolated according to:

$$Y_p \simeq \left\{ Y_{p(\beta_1=0)} + \left(\frac{\beta_1}{\alpha_2}\right)^2 \left[Y_{p(\beta_1=\alpha_2)} - Y_{p(\beta_1=0)} \right] \right\} \left(\frac{t/c}{0.2}\right).$$

$Y_{p(\beta_1=0)}$ is the loss coefficient for nozzle blades (blade inlet angle β_1 is 0) This is the case of the first stator of impulse turbine.

$Y_{p(\beta_1=\alpha_2)}$ is the loss coefficient for impulse blades ($\beta_1 = \alpha_2$ so blade inlet angle is equal to gas outlet flow angle). This is the case for the impulse turbine rotor.

60

The last term is a correction for t/c, the thickness to chord ratio.

When inlet flow angle is different from inlet blade angle and incidence is not zero, stall can happen as was the case for Wells turbine when angle of attack was increasing. The correlation gives a way of calculating the pressure drop in this situation (fig.3.14) in terms of a incidence coefficient to multiply by Yp (i=0).

$$k_i = \frac{Y_p}{Y_{p\ (i=0)}}$$

This coefficient is function of the ratio

$$\frac{i}{i_s}$$

-i is the incidence (flow angle minus blade angle)

-is the incidence which gives stall of the blade.
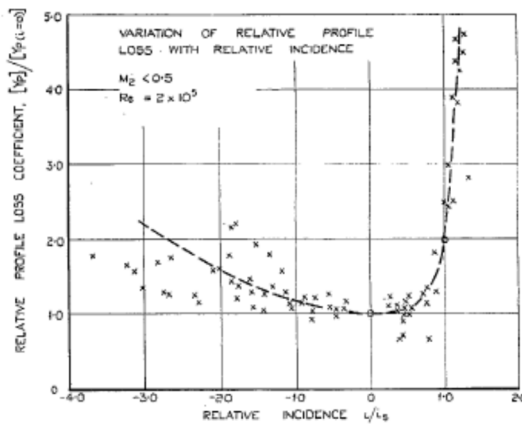

FIG. 8a.   Variation of loss and outlet angle with incidence.

Fig. 3-14:variation of loss coefficient with incidence

The plot in (fig.3.14) shows that for negative incidence, the drag region is reached, in which skin friction losses increases with respect to the case of zero incidence. For positive incidence, the stall region is reached, because of boundary layer separation.

In the Matlab code the interpolation of the curve is done using two polynomial: one for negative values of abscissa in (fig.3.14) and one for positive values. Relative incidence (abscissa in (fig3.14)) in the code is called "inc_r"; the interpolation is:

```
if inc_r>0
  c_loss_a=(0.15*inc_r^3+0.775*inc_r^2+0.075*inc_r+1)*c_loss_a;
  c_loss_a=c_loss_a;%+0.04;

  else if inc_r<=0
          c_loss_a=(0.1125*inc_r^2-0.0675*inc_r+0.9925)*c_loss_a;
          c_loss_a=c_loss_a;%+0.04;
```

Ainley Mathieson correlation gives a way to estimate the stall incidence (fig.3.15) for different values of :

$$-\frac{\beta_1}{\alpha_2} = \frac{blade\ inlet\ angle}{flow\ outlet\ angle}$$

$$-\frac{s}{c} = pitch\ to\ chord\ ratio$$
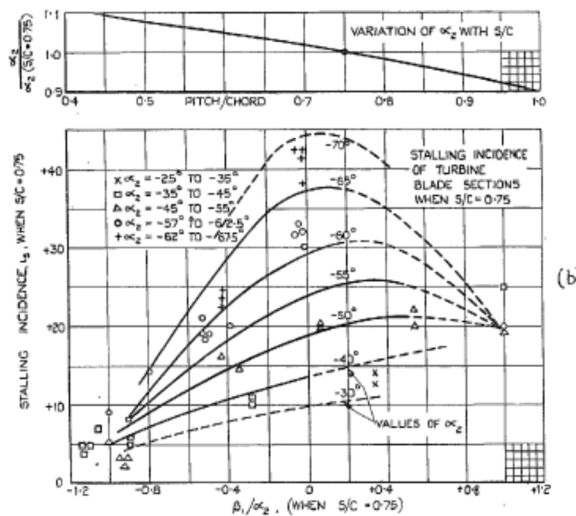
FIG. 7. Positive stalling incidences of cascades of turbine blades.
$Re = 2 \times 10^5$; $M < 0.6$.

Fig. 3-15:stalling incidence according to Ainley MAthieson

The correlation gives also other two corrective coefficients for different Re number and Mach number.

As far as the flow outlet angle is concerned, the correlation suggests that it tends to decrease by about 2% between zero incidence and positive stalling incidence, but no clear trend it is predicted for negative incidence.

Ainley Mathieson's correlation has shown to predict the behaviour of the first two rows with good accuracy, but for the third row, a different correlation has to be used, since the exit is axial, and with 0 angle at the outlet, the abscissa in the plot in (fig.3.15) is not defined ($\alpha_2=0$).

For the second stator, the situation is difficult to describe with a correlation found in literature, since the flow is coming toward the trailing edge of the blade and not towards the leading one, and the incidence can be outside the range usually defined in correlations;

It has been chosen to use Howell's correlation, generally used for compressors rows, since the second stator should act more like a compressor blade, than a turbine one.

HOWELL:

As for Ainley Mathieson, a loss coefficient is defined as a function of incidence
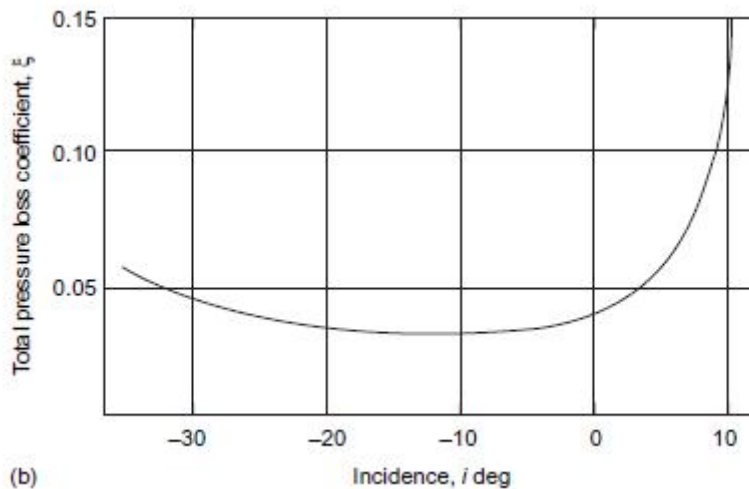

Fig. 3-16:pressure loss coefficient in nominal condition; taken from [6]

Knowing the camber θ (difference between inlet and outlet blade angles), Howell's correlation allows to estimate the deflection of the flow at the exit of the blade δ in terms of m, camber , space to chord ratio to the n power (0.5 for compressor cascade and 1 for compressor inlet guide vane). This estimate is done in the nominal condition, defined as the condition in which the deflection ε (difference between inlet and outlet flow angles) is 80% of the stalling deflection.

$$\delta^* = m\theta(s/l)^n,$$

$$m = 0.23(2a/l)^2 + \alpha_2^*/500$$

a/l is distance of maximum camber from leading edge.

With δ, the outlet angle is corrected and from (fig.3.17) nominal deflection ε is found (difference between flow angle at the inlet and outlet in nominal conditions). So inlet flow angle in nominal conditions is known. The nominal incidence is the difference between the flow inlet angle and the blade inlet angle.
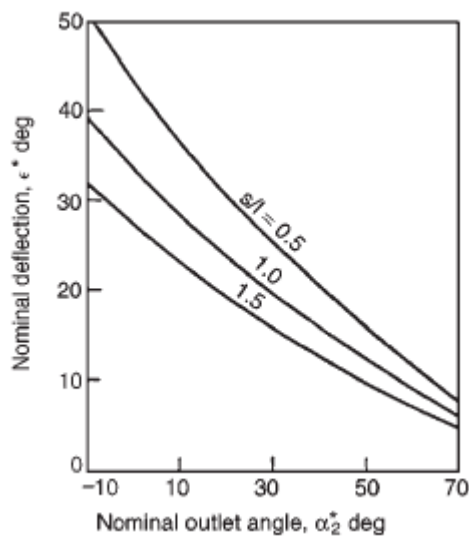

Fig. 3-17: nominal deflection; taken from [6]

From (fig.3.16) the loss coefficient for nominal condition is found. If the blade works in off design conditions in which the inlet flow angle is different from the one found by nominal deflection, the correlation gives a way to estimate off design deflection (fig.3.18):
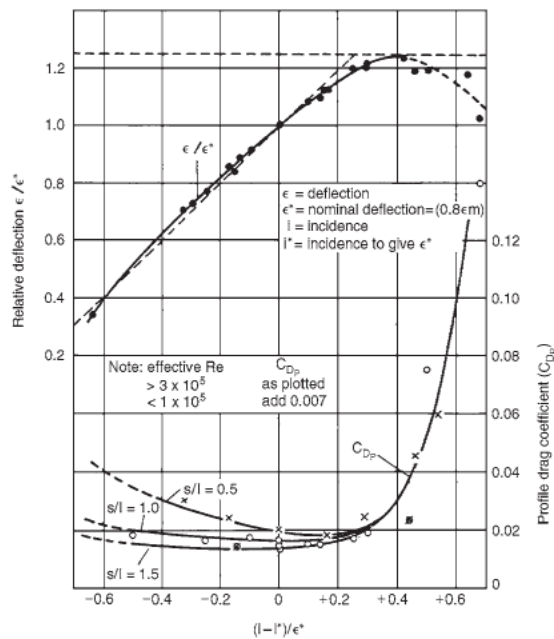
Fig. 3-18: relative deflection and drag coefficient for off-design conditions; taken from[6]

From off design incidence (flow angle in the particular off design condition -blade inlet angle) and nominal incidence and deflection, abscissa in (fig.3.18) is known, and off design deflection is calculated. From the same plot drag coefficient is calculated and using the following equation.

$$\zeta = \Delta p_0 / \left(\tfrac{1}{2}\rho c_x^2\right) = C_D / [(s/l)\cos^3 \alpha_m].$$

 the loss coefficient is estimated.

In the Matlab code, the interpolation used for the curve in (fig.3.18) is based as for Ainley Mathieson, on two polynomic, one for negative values of abscissa (xh in the code) and one for positive values;

```
if xh<=0

        Cdrag=1*0.0357*xh^2-1*0.0107*xh+0.0203;%+0.8*xh^2;
    else if xh>0
            Cdrag=1*1.875*xh^4-1.2083*xh^3+1*0.3396*xh^2-
1*0.0408*xh+0.0201;
```

ZWEIFEL CRITERION:

As far as the number of blades is concerned, Zweifel's criterion has been used to calculate the optimal number of blades:
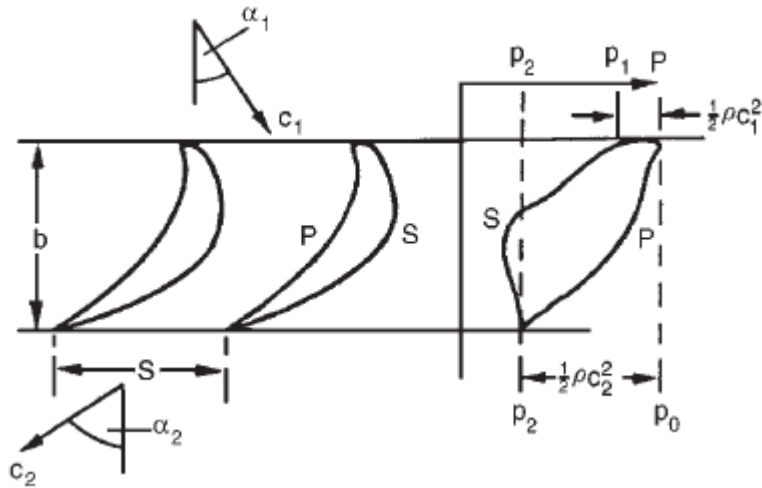
65

Fig. 3-19:control volume for Zweifel criterion; taken from [Dixon, Fluid Dynamics and thermodynamics of turbomachinery, 5th ed.]

From tangential momentum balance applied to the control volume in (fig.3.19),

$$F_y = \rho \cdot s \cdot v \cdot (v_{y1} - v_{y2})$$ (3.10)

This tangential force is also called blade loading. The ideal loading is the one in which the maximum pressure on the P side is the whole stagnation pressure at the leading edge kept constant for the length b, and the minimum pressure is the total stagnation pressure (which is conserved) minus dynamic pressure at the outlet:

$$F_{ideal} = b[p0 - \left(p0 - \frac{1}{2}\rho v_2^2\right)]$$ (3.11)

The ratio of blade loading (3.10) and optimal blade loading (3.11), according to Zweifel should be 0.8 to minimize the losses; this gives a way to choose space to chord ratio, and so the number of blades, if the chord is known.

After some manipulation with triangles of velocities, the ratio becomes:

$$\psi = 2\frac{s}{b}(\cos \alpha_2)^2 (\tan \alpha_2 - \tan \alpha_3)$$

66

3.4 1D MATLAB CODE:

For the preliminary design of impulse turbine, a code in Matlab has been written: the design axial velocity is 20 m/s, to compare the behaviour of Wells and Impulse turbine.

The code finds and optimal design, as was done for Wells turbine, making calculations for each flux number ϕ and solidity, especially calculating the pressure drop, and then, after having excluded the solutions outside the pressure drop range, comparing the solutions to choose the best efficiency one. There are however more parameters that have to be optimized with respect to the Wells turbine case, mainly the angles of the blades:

$-\alpha_2$: outlet blade angle of the first stator and inlet blade angle of the third stator

$-\beta_2$: inlet and outlet blade angle of the rotor

What has to be found is the optimal combination of these, that leads to the most performing turbine in terms of efficiency.

 The code is organized in this way: there is a Main Program that takes a fixed chord length, and for the values of the rotor inlet angle in a range [20° 70°] it calls a function "Impulse.m". This function "Impulse.m" uses correlations and Zweifel criterion to design the turbine for all the values of phi in the range [0.05 4] and ultimately gives back to the main program the best design in terms of efficiency. The main program then, compares all the efficiencies coming from different rotor blade angles, and select the highest one.

In this way optimization is done in two moments: optimization with respect to phi is done by the function "Impulse.m", while optimization with respect to rotor blade angle is done by the main program.

To make calculations with a different chord length, the main program has to be run again from the beginning with the new chord length value. In the following, the detailed working of the function "Impulse.m "is explained.

FUCTION "IMPULSE.M"

The function takes as fixed the following parameters:

-chord length

-β_{2b}: inlet and outlet blade angle of the rotor

The function "Impulse.m " has the role of finding for a fixed rotor angle and chord length the value of ϕ that gives best efficiency. The function performs the following calculations for every phi in the range [0.05 4] and choose the one that gives maximum efficiency and at the same time gives a pressure drop inside the range of 1000 Pa +/- 5%. Since the pressure drop correlations require knowlege of the blade angles, number of blades, and the velocities at outlet of every blade row (which are not known at the beginning), an iterative procedure has to be performed.

Everything starts from v_{t2}:

from Euler equation (3.1)

$$P = \rho \cdot A \cdot v \cdot u \cdot 2w_{t2}$$

Using definition of efficiency (0.2) it is possible to write:

$$\eta \Delta p_t \cdot Q = \rho \cdot A \cdot v \cdot u \cdot 2w_{t2}$$

which becomes, after simplification,

$$\eta \Delta p_t = \rho \cdot u \cdot 2w_{t2}$$

Remembering that from triangle of velocity $v_{t2} = u - w_{t2}$,it is found:

$$v_{t2} = u + \frac{\eta \Delta p_t}{2 \cdot \rho \cdot u}$$

ϕ is fixed at the beginning of the calculation, so u is known, total pressure drop is not known, but for simplicity Δp_t is imposed to 1000 Pa, the required pressure drop. Since blade velocity in impulse turbine is not high [13] , rotation of the wake is negligible and static and total pressure drop can be considered to be equal.

Efficiency and number of blades are not known, and they are firstly assumed, to start calculations.

STATOR 1

From v_{t2} and u, v velocities, through trigonometry it is possible to solve the first triangle of velocity, and knowing the velocities at the outlet of the first stator, it is possible to calculate the pressure drop with Ainley Mathieson's correlation.

ROTOR

Outlet conditions of first stator are inlet for the rotor: the exit triangle is calculated imposing outlet flow angle equal to the blade rotor angle, so that also triangle of velocity at the outlet can be solved knowing outlet flow angle beta3, u, v. Knowing velocities at inlet and outlet of rotor, the pressure drop is calculated using Ainley Mathieson. A new optimal number of blades is calculated using Zweifel criterion; this new number of blades will be used in the subsequent iteration.

STATOR 2

Knowing inlet velocities at second stator and also at the outlet (it is assumed $v_4 = v_1$), it is possible to calculate pressure drop at the second stator with Howell's correlation.

Summing up the pressure drops, the pressure drop between inlet and outlet is found; power extracted is calculated by means of Euler equation (3.1) and ultimately efficiency using (0.2)

Once the efficiency and the optimal number of blades are calculated, they are inserted back at the beginning to make iterations until convergence to some values of efficiency and pressure drop is found.

In a similar way the code performs this calculation for other phi in a range [0.05 4] and build a vector in which results are stored with one condition: that the pressure drop is inside the ranges of 1000 Pa +/- 5%.

Finally the function search in this vector which is the best efficiency solution.

MAIN PROGRAM "Impulse_turbine.m"

The solution found by the function"Impulse.m" is valid only for a single rotor blade angle, so the role of the main program is to call the function to give results for a range of rotor blade angles, and for each one to give the best solution with the relative ϕ value.

The results given by the main program are given in form of a plot of efficiency as a function of rotor inlet blade angle. To investigate the effect of different chord lengths, the main program has to be run again, giving a different plot of efficiency as a function of rotor inlet blade angle.

RESULTS:

The Matlab code results are reported (fig.20) for a chord length of 0.3 m since it is the one that guarantees the best efficiency. It exist a maximum of the rotor blade angle that maximizes efficiency. This value is 52°.
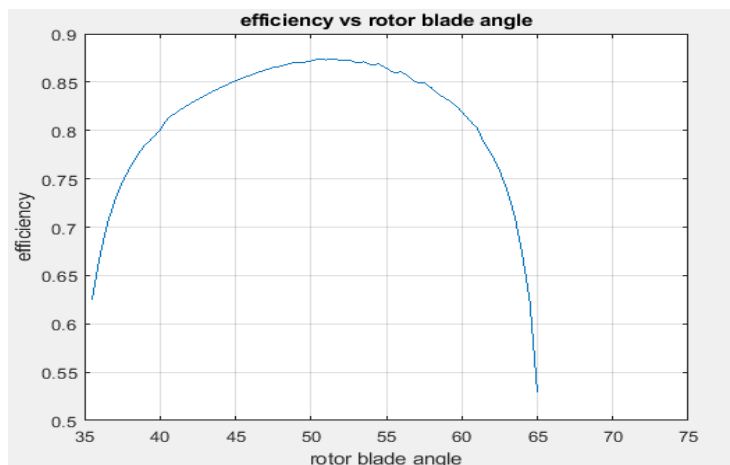

Fig. 3-20: efficiency as a function of rotor angle blade angle according to matlab code

For this maximum, the corresponding machine parameters are:

efficiency	0.874
phi	1.25
number of blades	38
u velocity [m/s]	16
alpha 2 [°]	62.8
beta 2 [°]	49
alpha 3 [°]	24.5
beta 3 [°]	52
pressure drop [Pa]	1045
Force [N/m]	141.5

Fig. 3-21: best solution according to Matlab

According to simple calculations, expressing pressure losses as in (3.7), optimal configuration should have β_3 and α_2 equal to each other but in the Matlab code there is a difference of 10°.

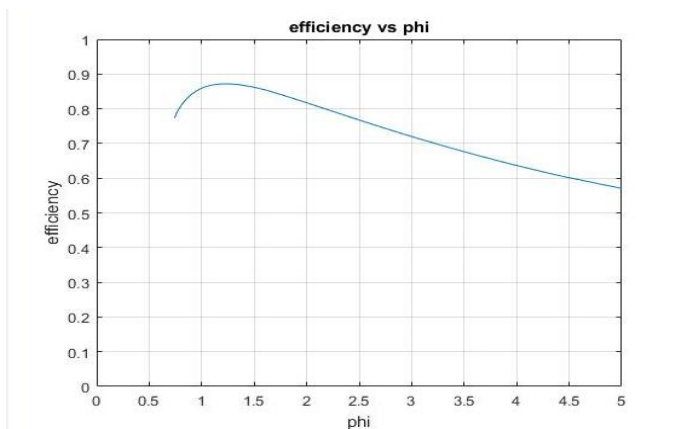Efficiency as a function of phi for the best solution in (fig.3.21) is plotted in (fig.3.22)

Fig. 3-22: Efficiency as a function of phi for the solution in (fig.3.21)

In (fig.3.23) the loss coefficents are reported as a function of phi;
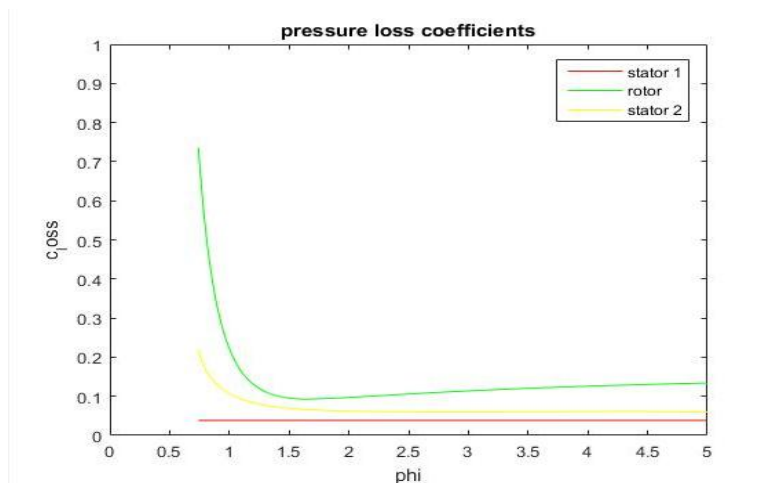
Fig. 3-23: loss coefficients as a function of phi for the solution in (fig.3.21)

The hypothesis of assuming the loss coefficients constant with respect to phi, as was done in (3.7), is wrong when phi becomes lower than 1.5 . For lower phi, the coefficients start growing, increasing the pressure drop and decreasing efficiency.

The fact that loss coefficients grows for lower phi is due to the correlations used: When u increases (phi decreases), difference between flow and blade rotor angle increases and the abscissa in Ainley Mathieson (fig.3.14) moves to the left, moving into the high drag losses. The same is true for Howell's correlation at the second stator: when u increases also difference between flow and blade stator angle increases and the abscissa (fig.3.18) moves to the left into the high drag losses region. Flow separation and recirculation occur both at the stator and the rotor.

The turbine is strongly limited by drag losses in the low phi region, so that rotational velocity has to be limited.

It has to be underlined that these results strongly depend on the correlations used: the second symmetric stator especially, is hard to model in terms of a correlation for pressure drop, because it's not a usual part of turbines and there are no correlations that fits to it correctly to check the results, CFD simulations have been done.

In the next paragraph, a 2D model based on CFD calculations to validate the 1D model is presented;

3.5 2D MODEL:

Since Matlab code was performing calculations based on velocity triangles and correlations, no reference to the type of blade profiles used appear in 1D calculations.

But to perform CFD calculations a choice has been done. For the rotor, circular and elliptic profile are usually the choices; according to experiments done by [13], elliptic profiles are superior to circular ones and the optimal blade rotor angle is about 60°, not very far from the 52° angle predicted by preliminary 1D design. They also suggest that the optimal t/s as defined in (fig.3.24) is 0.4.
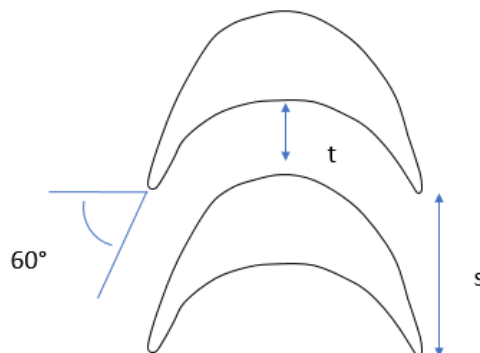

Fig. 3-24: t/s ratio for rotor angles

In the CFD model, only elliptic profiles have been tested.

As far as the stators are concerned, two solutions are possible: airfoil type profiles as in (fig.3.1) or plane type as in (fig.3.27). Always in [13], it is suggested that the optimal angle of the stator blades it's 60°; the fact that both stator and rotor angles are equal agrees with theoretical analysis represented in (fig.3.10), even if theoretical analysis was simplifying pressure loss coefficients considering them constant.

The geometric domain chosen to perform simulations, is similar to the one used for Wells turbine in chapter 1, with three parts built to perform frozen rotor calculations.

The mesh used for calculations consists of three parts divided by internal interfaces: a fixed inlet and outlet part and a moving central part (fig.3.25). A zoomed view of the mesh around the blades is given in figure (3.26) The inlet is modelled with a velocity inlet boundary condition that imposes an axial velocity v=20m/s ; the outlet is modelled as a pressure outlet boundary condition with 0 relative pressure. Periodic boundary conditions are used to take into account the presence of neighbouring blades. The mesh consists in about 43000 cells.
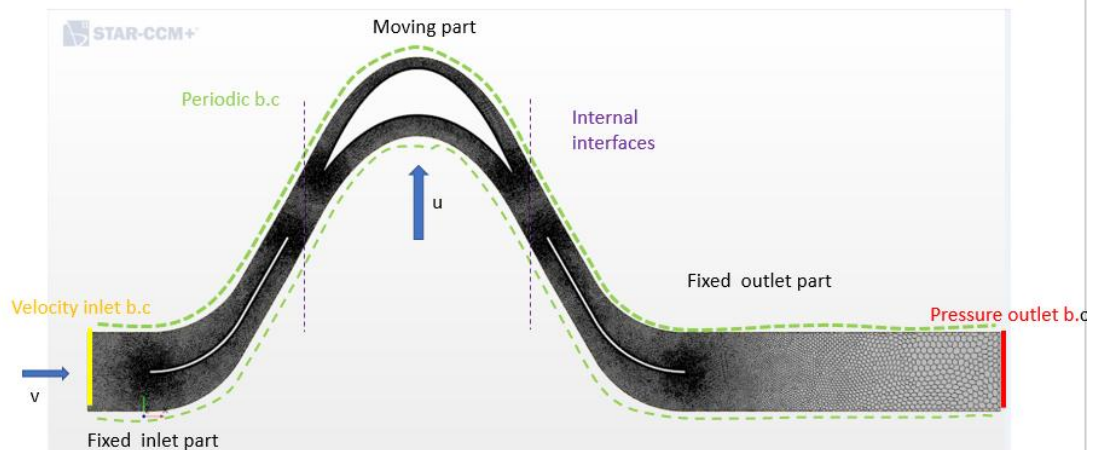

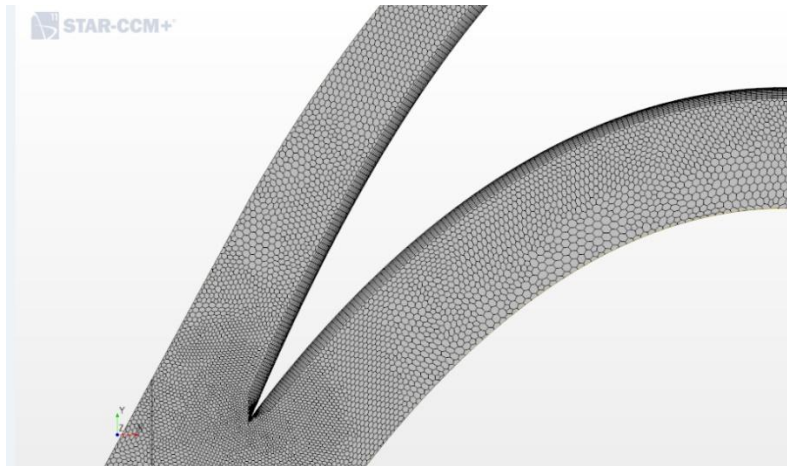*Fig. 3-25:mesh used for impulse turbine*

Fig. 3-26:zoom on rotor blade in the mesh

Mesh independence tests have been done to make sure that increasing the number of cells leads to a determinate value of the calculated quantities. An example is given in (fig.3.27)
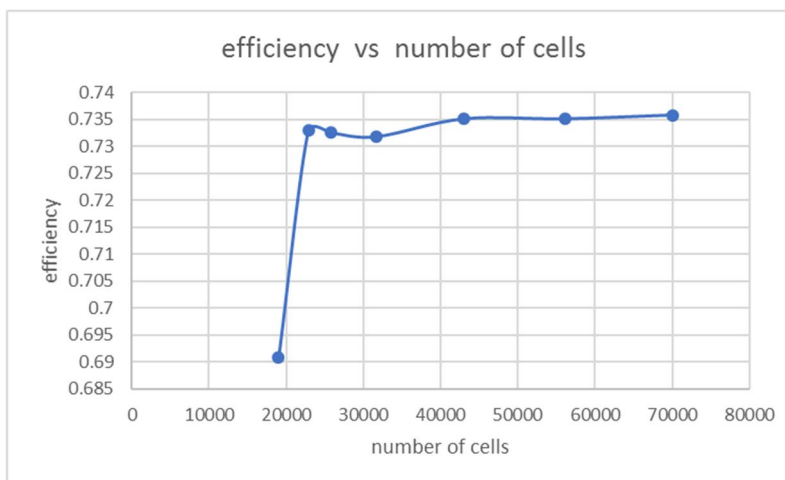

Fig. 3-27: effect of number of cells on convergence for mesh

The physical model chosen in Star-CCM+ for Impulse turbine is represented by the following equation:

- Continuity equation
- Reynolds averaged Navier-Stokes equations
- Turbulent kinetic energy eqn
- Turbulent dissipation rate eqn

- Substance state equation (constant density)

For impulse turbine, since blade velocities are much lower than for Wells turbine and comparable with 20 m/s, the Mach number is expected to be less than 0.3 (corresponding to a velocity of 105 m/s) so a constant density state equation has been chosen instead of ideal gas model since it permits to avoid solving the energy equation, and so it allows to perform faster calculations without loosing in precision. The turbulence model chosen is k-ϵ.

NACA PROFILE:

The 2D model just described has been first used to make a simulations with NACA 0012 for the optimal case according to 1D calculations and the cases of rotor blade angle corresponding to 45° and 55° .

It has been noted that flow angles at the outlet of the stator and rotor are different from blade angles. Flow angle at the outlet of the stator in all the simulations has shown to be between 5° and 9° less than the blade angle; this tells that NACA profile have poor ability to guide the flow. Flow angle at the outlet of the rotor is +/- 3° the blade angle.

It has also been noted that the correlations underestimate pressure loss coefficients and so pressure losses, with the consequence that efficiency predicted by 1D model is higher than the actual one predicted by 2D model. In particular:

-Ainley Mathieson slightly underestimates loss coefficients and pressure drop: it predicts pressure drop at the first stator with an error of less than 5%. As far as the rotor is concerned Ainley Mathieson predicts the shape of the pressure drop curve, with a maximum error of 24% for u velocity of 20 m/s and a minimum one of 2% for 7.5 m/s.

 -Howell's correlation predicts the shape of the pressure drop curve but underestimates the values with an error of more than 50%. A correction of Howell's correlation should be done, but in the present work nothing of this kind was done.

Some simulations have been performed in an interval of rotor blade angle around 52° and it was seen that the best efficiency is reached for a configuration of [stator blade angle° rotor blade angle°]= [66° 60°]. The efficiency for this configuration is plotted in (fig.3.28) and the pressure drop in (fig.3.29).
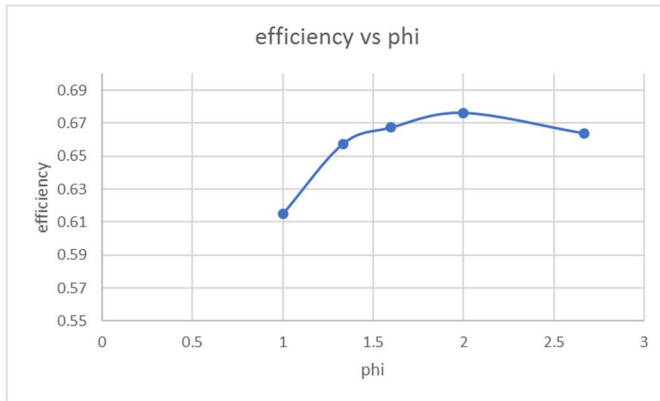

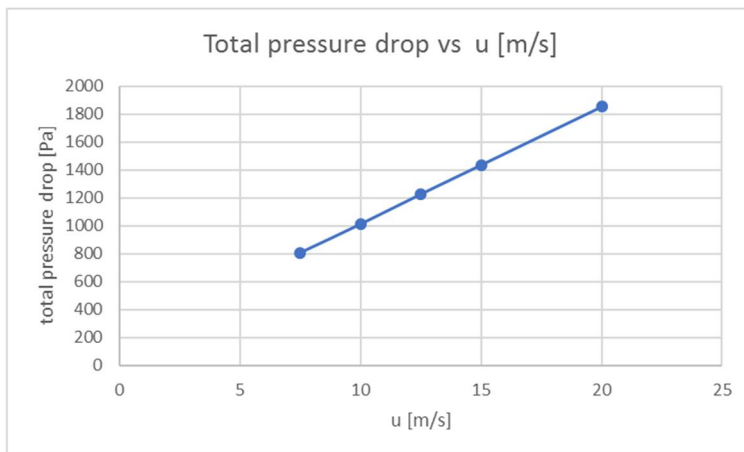*Fig. 3-28: efficiency as a function of phi for [66° 60°]*

Fig. 3-29 pressure drop as a function of phi for [66° 60°]

The efficiency for this configuration is actually higher than for other rotor angles also for lower number of blades. In the following, three simulations for 30 blades and increasing stator and rotor angles are reported:
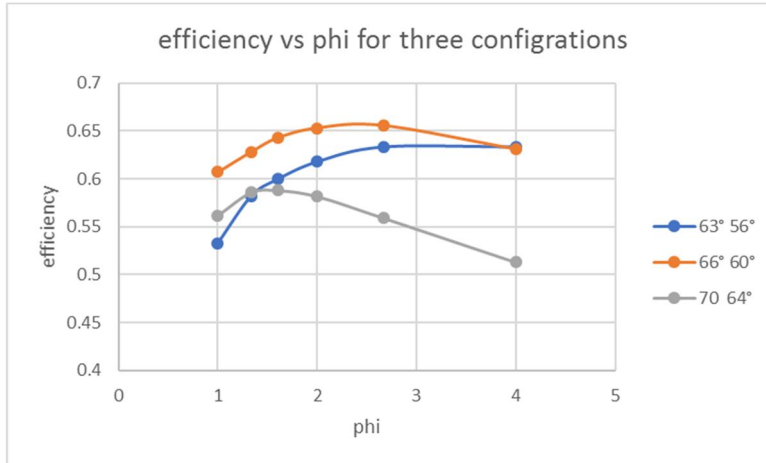
-64 °56°

-66° 60°

- 70° 64°

Fig. 3-30: efficiency vs phi for 3 configurations

The results show that increasing the angles does not increase efficiency, infact it decreases it, as Matlab code suggested, even if Matlab code was predicting best efficiency for a blade rotor angle of 52°.

The configuration [60° 60°] was simulated for 40 blades: peak efficiency is 0.66, (fig 2.39) slightly lower, than 0.676 for [66° 60°]. The reason is that because of angle deviations at the exit of the stator of about 6° or 7°, the actual angle it is not 66° but 60° while for [60 60°] configuration, with a deviation of 5°, the actual outlet stator angle is 55°. With NACA profiles, the exit angle from the first stator is always lower than the blade one, and this is one of the main reasons of lower efficiencies than 1D predicted.

PLATE PROFILES:

Simulations have been done also for the plate type profile, for the same angle configurations tested for NACA profiles and also for the configurations [50° 50°], [55° 55°], [70° 70°], since according to (3.10), best solutions have equal stator and rotor angles.

It was seen that the profile in figure (fig.2.31) is superior since it guides the flow better and there is no actual angle deviation at the outlet of the first stator. The best efficiency configuration with plate type profiles has been shown to be [60° 60°].
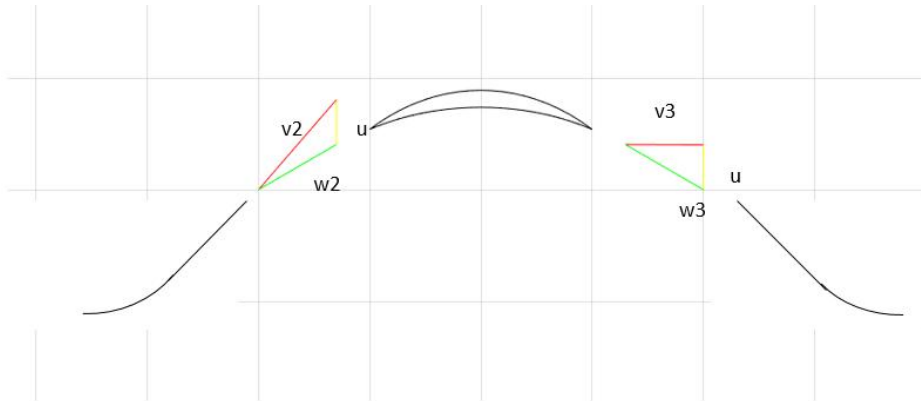
For the same configuration of [60 60°] and the NACA profiles, efficiency and pressure drops are compared for the case of 40 blades in figures (fig.3.33) and (fig.3.34):

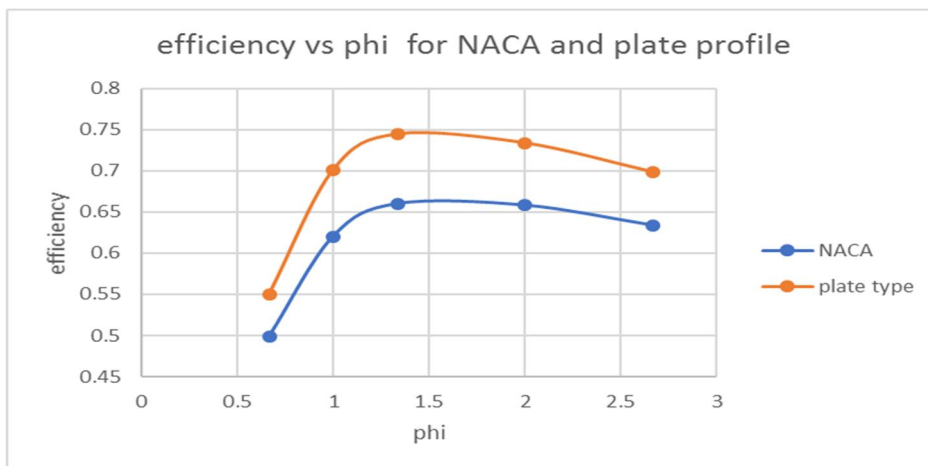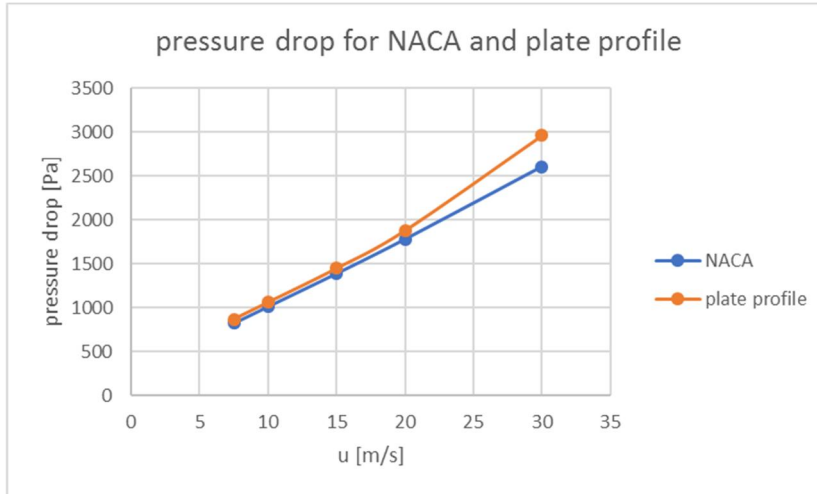Fig. 3-33:pressure drop for NACA and plate profiles for [60° 60°]

Efficiency is higher with plate type profile: this is due to the fact that plate type profile can better guide the flow creating bigger velocities at the outlet of the stator, which is beneficial for power extraction looking at (3.1). This can be seen in the CFD scenes for plate type and blade profiles in figures (fig.3.35) and (fig.3.36).
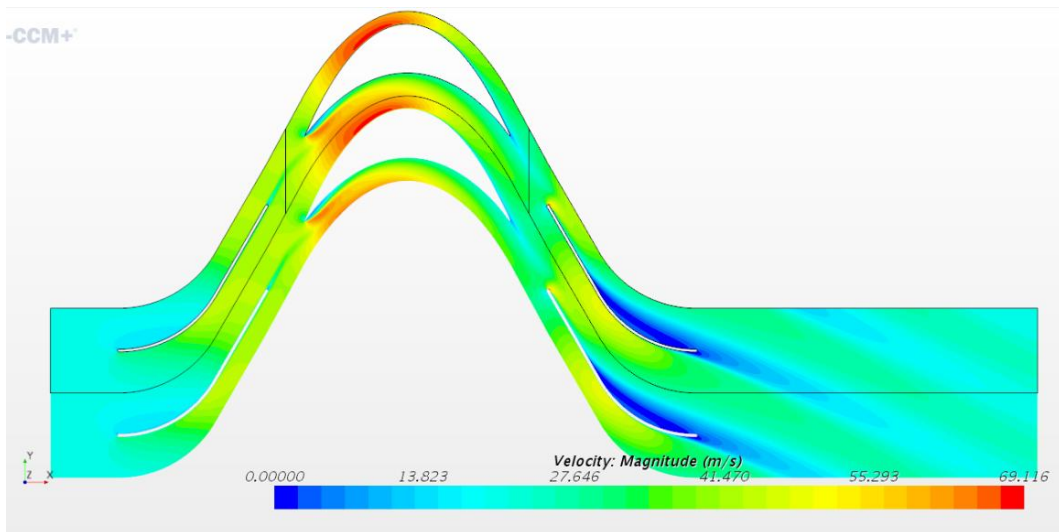

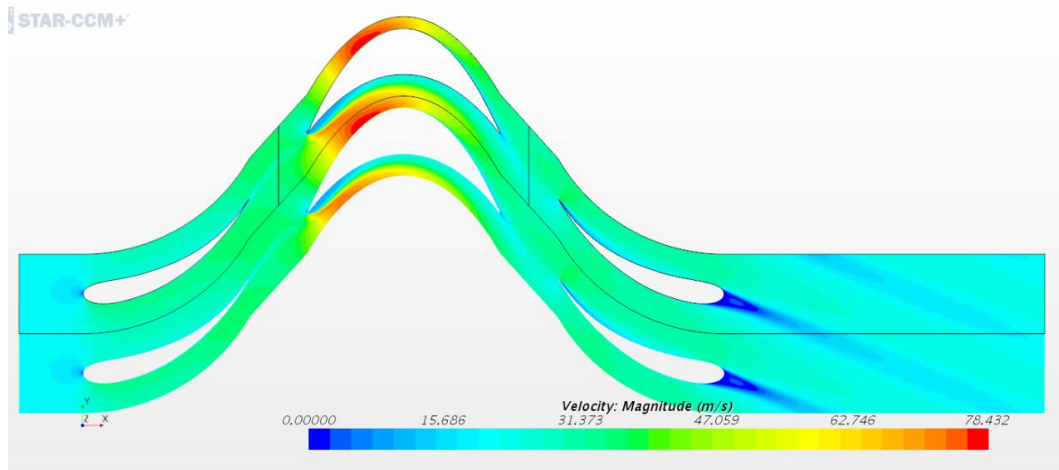Fig. 3-34: velocity distribution for plate type [60° 60°]

Fig. 3-35:velocity distribution for NACA [60° 60°]

Velocity at the outlet of the stator is higher in the plate type case (fig.3.35). In the case of NACA, the 60° degrees are met just in the last part of the blade, but this last part of the blade cannot overcome inertia forces that would tend to keep the flow axial; in the case of the plate type, for the same chord length, more part of the blade is at 60° to impose a 60° turn to the fluid.

If the [66° 60°]solution is tested for plate type and u=10 m/s, peak efficiency drops down at 0.57. This corresponds to the situation in which no incidence angle at the rotor is found, as can be seen from (fig.3.38), and high pressure losses are found in the second stator.
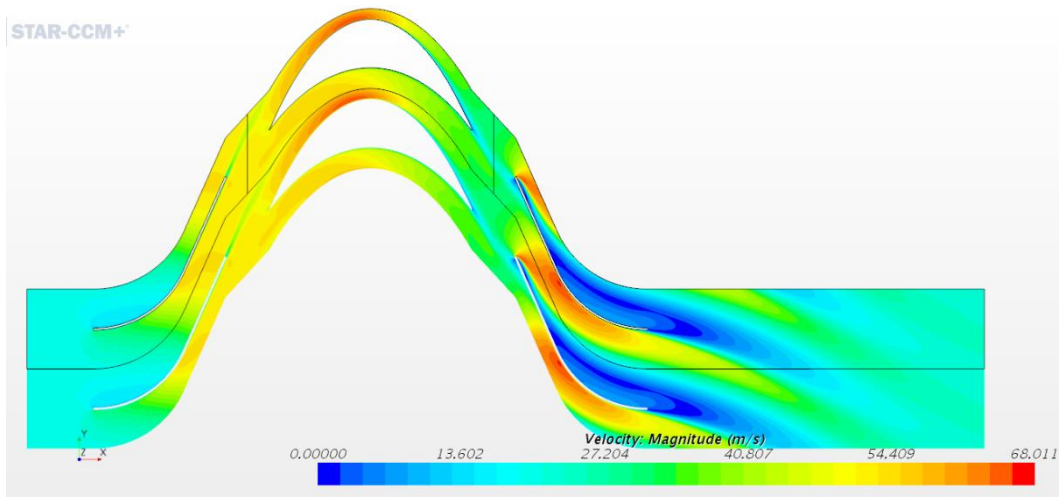
Fig. 3-36: Velocity distribution for [66° 60°]

As can be seen from the pressure drop values for this configuration in (fig.3.40), and efficiency values in (fig.3.39), efficiency decreases because pressure drop is higher than in the [60° 60°] case.
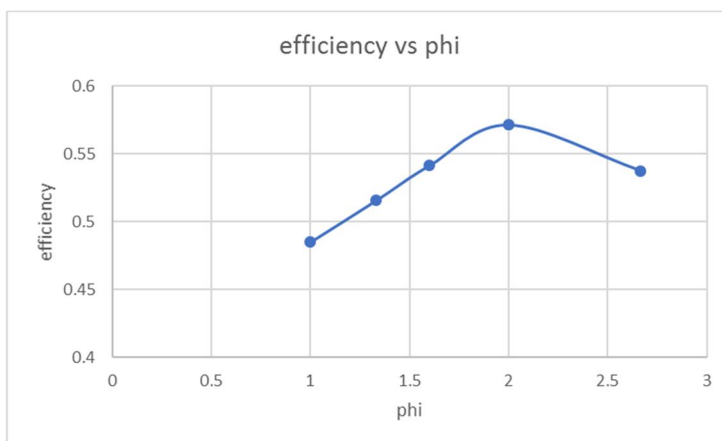

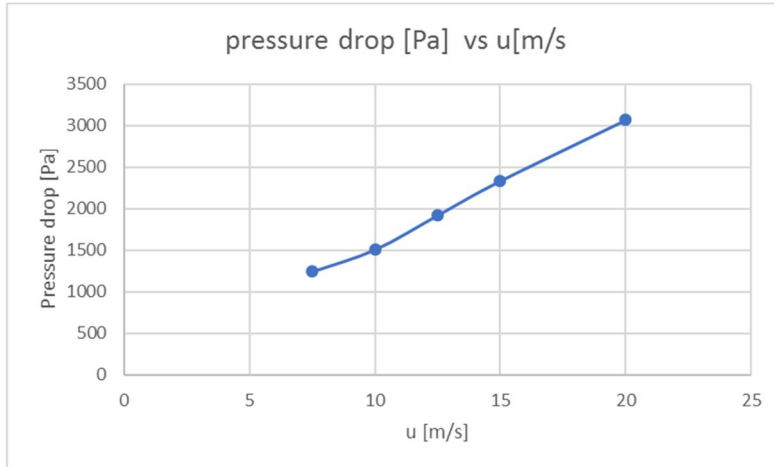*Fig. 3-37: Efficiency vs phi for [66° 60°]*

Fig. 3-38: Pressure drop vs u [m/s] for [66° 60°]

The configuration [60° 60°] has been chosen for design. Keeping these blade angles, it was also tried to study the effect of solidity.

EFFECT OF SOLIDITY:

Different solidities have been tested (fig.3.39) for the [60° 60°] configuration at u= 15 m/s, the blade velocity at which the maximum efficiency is found (fig.3.33)

solidity	0.2	0.3
30	1.273885	1.910828
40	1.698514	2.547771
50	2.123142	3.184713
60	2.547771	3.821656

Fig. 3-39: Solidity tested for the [60° 60°] case

Pressure drops for the various solidities are reported in (fig.3.40). The effect of solidity on pressure drop is limited.

delta p	0.2	0.3
30	1733	1446
40	1558	1446
50	1459	1769
60	1511	

Fig. 3-40: Pressure drops corresponding to the tested solidities

If efficiency is considered (fig.3.41), the solution with chord length

of 0.2 is less efficient, and highest solidity corresponding to 50 blades and c=0.3m and lowest solidity corresponding to 30 blades and c=0.2m are the least efficient.

eta	0.2	0.3
30	0.380401	0.650818
40	0.576437	0.744421
50	0.67667	0.616599
60	0.676567	

Fig. 3-41: Efficiencies for the tested solidities

The solution for design is chosen with a chord length of 0.3 m and 40 blades, and with a rotational velocity of 10 m/s, since 15 m/s gives pressure drops outside the required range irrespective of the solidity. If 10 m/s is chosen, efficiency is 0.733, very close to the maximum of 0.74 found at 15 m/s .The design parameters for Impulse turbine are represented in (fig.3.42):

ϕ	2
u [m/s]	10
stator blade angle	60°
rotor blade angle	60°
blades	40
chord [m]	0.3
Power [kW]	36.6
delta p [Pa]	1052
efficiency	0.733
solidity	2.54

Fig. 3-42: Design parameters of Impulse turbine

Velocity and pressure distributions are reported for this configuration in figures (fig.3.43) and (fig.3.44):
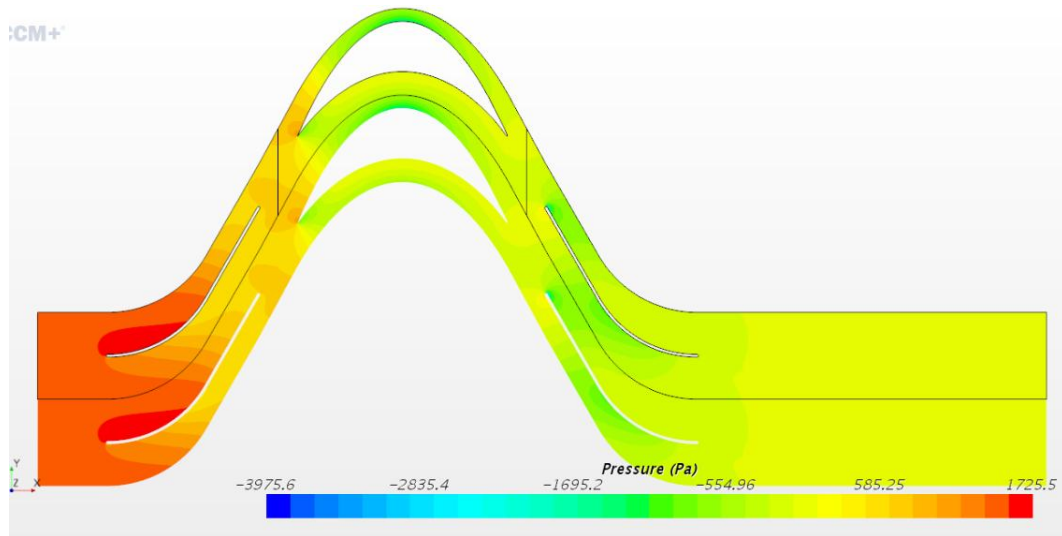
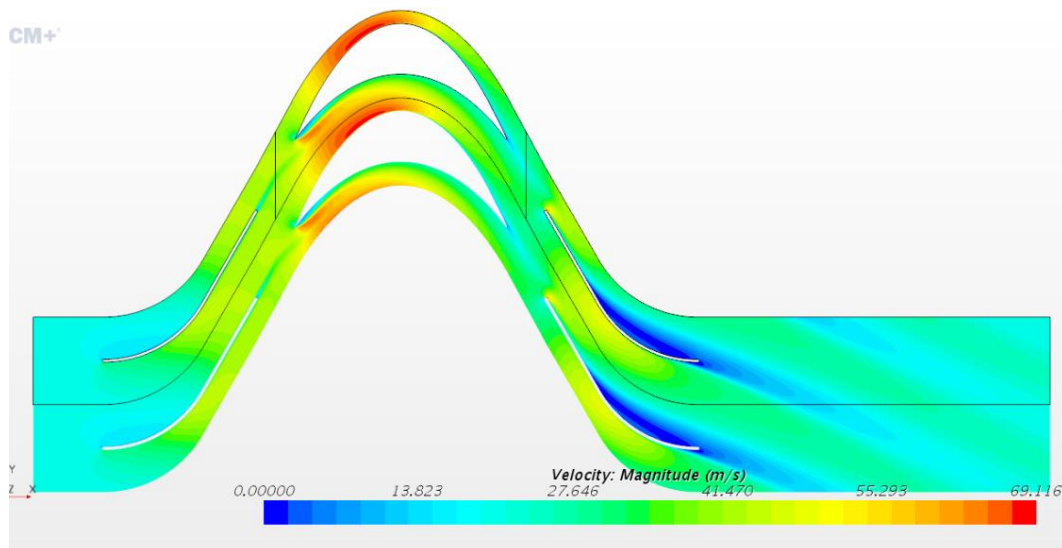*Fig. 3-43: pressure distribution for design solution*

Fig. 3-44: velocity distribution for design solution

3.6 OFF DESIGN PERFORMANCE:

Since during operation the turbine has to face different air flow conditions than the 20 m/s design one, the steady state behaviour of the machine chosen as the best solution (fig.3.42) has been tested for different air flow velocities. Different simulations have been carried out for a tangential velocity u of 10 m/s with a different air flow absolute velocity: power and efficiency curves for different air flow velocities are represented in (fig.3.45) and (fig.3.46).
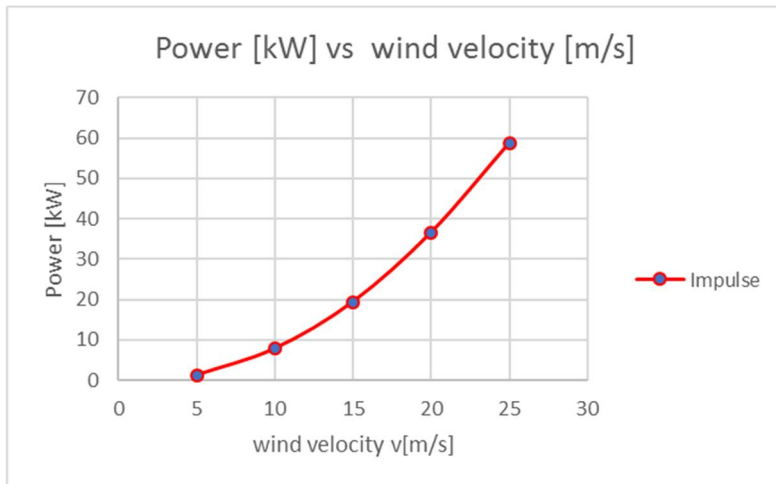
85
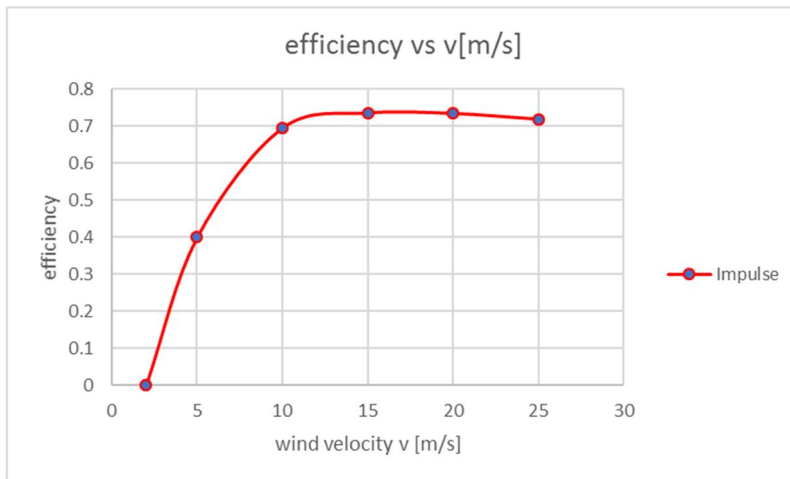
Fig. 3-45:power curve for Impulse turbine

Fig. 3-46: efficiency curve for Impulse turbine

4 COMPARISON OF THE TWO TURBINES:

To choose which turbine is the best solution for the application, a full 3D analysis of the turbine should be done, and also an unsteady analysis of the behaviour of the turbines subjected to the strongly unsteady air flows in the tunnels.

 Since this work only concentrates on 2D steady state analysis, some arguments that can help for the choice are reported, leaving more advanced analysis for a future work.

The first argument based upon which it is possible to make a comparison between the two turbines is the range of working condition, which is basically expressed by phi:

OPERATIVITY RANGES:

Efficiency as a function of ϕ is reported for the two turbines in (fig.4.1):
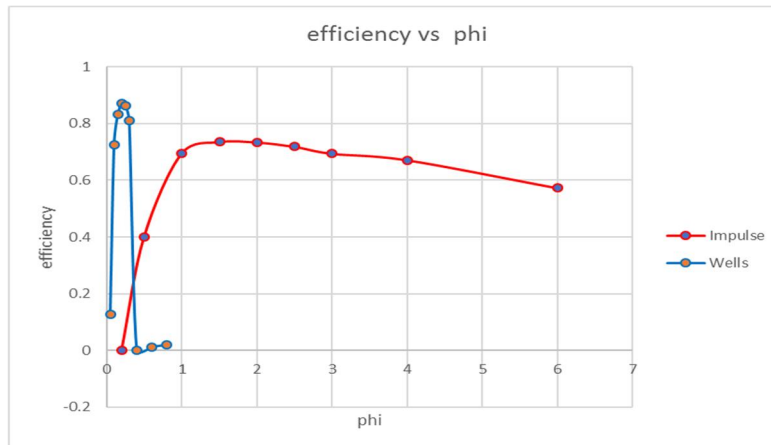

Fig. 4-1: efficiency as a function of phi for the two turbines

It is more useful for a comparison however, to express the curves as a function of a

$$\phi_r = \frac{\phi}{\phi_{maximum\_efficincy}}$$

In which $\phi_{maximum\_efficincy}$ is the ϕ at which the maximum efficiency occurs for each turbine. If the scaling is done, the plot becomes the one in (fig.4.2):
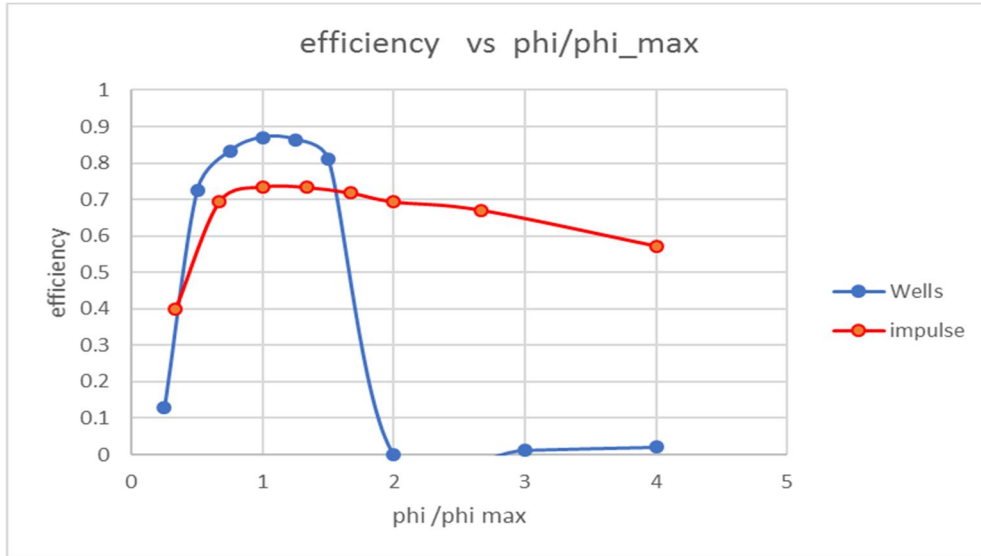
87

Fig. 4-2: Efficiency as a function of phi/phi_max

For Wells turbine, the working range is much smaller than for Impulse; acceptable operation is between ϕ_r =[0.5 1.5] and the main limitation is stalling occurrence at ϕ_r=1.5. After this point efficiency drops down becoming 0 for ϕ_r=2.

For ϕ_r of 3 and 4 however, efficiency is not 0, a sign that some power is produced. This is a consequence of the fact that force coefficient Cy, after stall has occurred, drops down, becoming negative, but as angle of attack is increased even further (bigger ϕ),it beguins to rise, as can be seen from (fig.4.3).
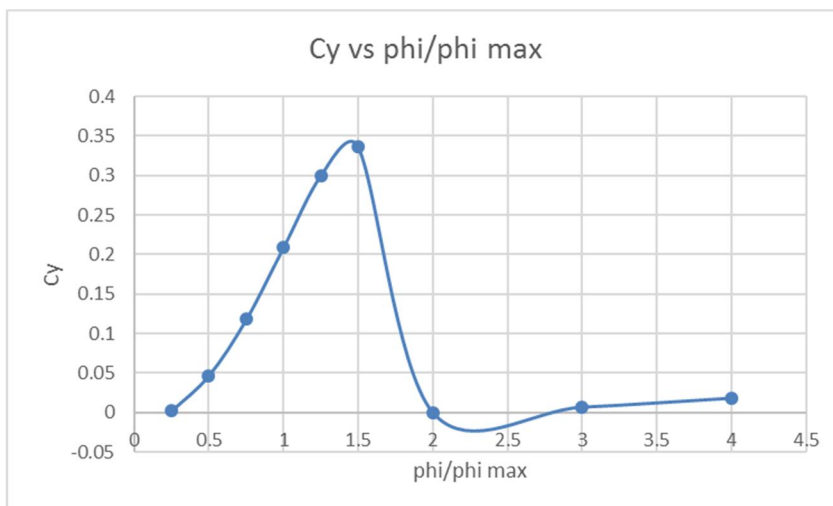

Fig. 4-3: cy coefficient as a function of phi/phi_max

This does not happen for Impulse turbine: no stall happens in the considered range, and the limitation for low ϕ values due to shock losses, and reduced force on the

blades. To compare force coefficients, a force coefficient is defined in the same way it was defined for Wells turbine:

$$c_F = \frac{F}{\rho \cdot (v^2 + u^2) \cdot c \cdot b}$$

Where b is the length of the blade; to work in two dimensions, b is assumed 1m. In (fig.4.4) force coefficient for Impulse is represented:
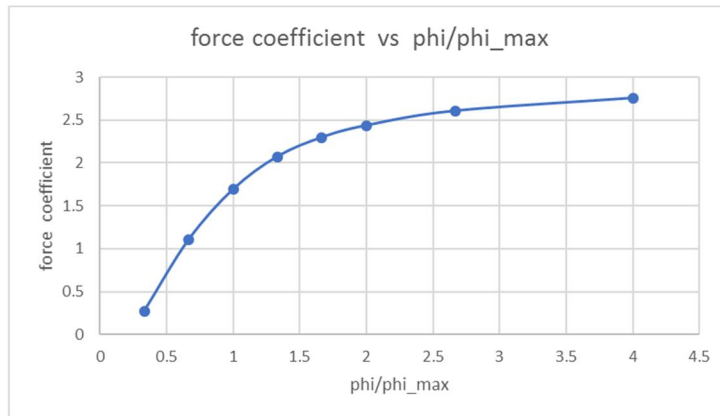

Fig. 4-4:force coefficient for Impulse turbine

If the Wells turbine start from 0 velocity (90° angle of attack and phi that tends to infinity) positive torque is produced, and the turbine starts to rotate, so u increases. But the more u increases, the turbine moves in the small or even negative force coefficients (phi between 2 and 3 in (fig.4.3)) until no torque is produced and the turbine does not accelerate to higher u velocities that would guarantee good operational range. The phenomenon in which the turbine cannot reach the design velocity is called crawling, and it is the reason why the Wells turbine is not self-starting. To bring the turbine in the good operating region, the electrical generator has to work in motoring mode to provide the starting torque.

To do this, electrical generators, usually induction generators, that can easily work also in motoring mode, are equipped with power electronics converters that are able to control the electrical torque of the machine to adjust the rotational velocity as desired using power tracking control algorithms.

This type of control should be faster as in the application considered in which strong velocity gradients are present in the tunnels. A faster and elaborate control is possible but of course it is expensive, also if considered that many machines are present working in different wind conditions in different parts of the tunnel, requiring separate velocity control.

For impulse turbine, no starting problems are present; to make use of all wind velocities, rotational velocity should not exceed the value corresponding to ϕ=0.5, because efficiency drops down, but there are no lower limits to rotational velocity, because the turbine can operate with good efficiency even for low rotational velocities for the whole range of wind velocities.

Velocity control is not a big issue for Impulse turbine as for Wells turbine and no velocity control could be done if the intent is to have a cheap solution.

As far as operating range is concerned, Impulse turbine is superior to Wells turbine since it doesn't require an accurate control of velocity which costs in terms of power electronics and electrical drives.

ROTATIONAL VELOCITY:

Impulse turbine works well with lower rotational velocities than the Wells turbine: this should have as consequences lower noise level production, and less mechanical stresses on bearings.

As far as noise production is concerned, [14] have done some experiments on some machines keeping axial velocity constant and varying rotational speed, and have found that sound power is proportional to $T^2 \cdot \omega$ and , for a fixed $T^2 \cdot \omega$ loud level produced by Wells turbine (WT in fig.4.4) is bigger then for Impulse (ITFG).
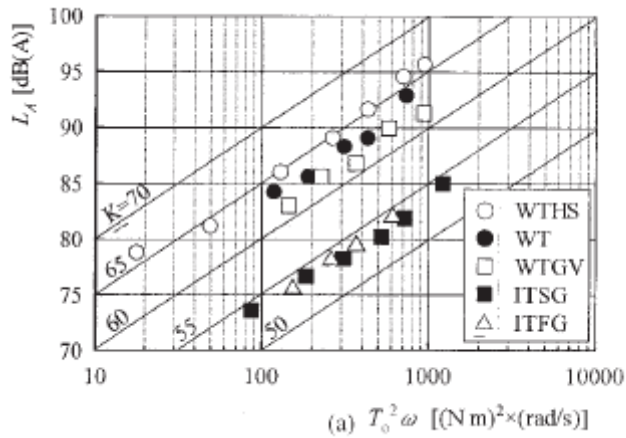
Fig. 4-5: loud levels for different turbines; taken from [14]

In the case of this application, the product of $T^2 \cdot \omega$ is:

- 14 (N m)^2 rad/s for Wells turbine with 76 dB(A)
- 101 (N m)^2 rad/s for Impulse with 75 dB(A)

Another source of problems related to rotational velocity are centrifugal forces which are bigger in Wells turbine because of higher operating rotational velocities.

AXIAL THRUST:

One more disadvantage of Wells turbine, are higher axial loads compared to Impulse turbine. In (fig.4.5) axial thrust is plotted as a function of ϕ_r.
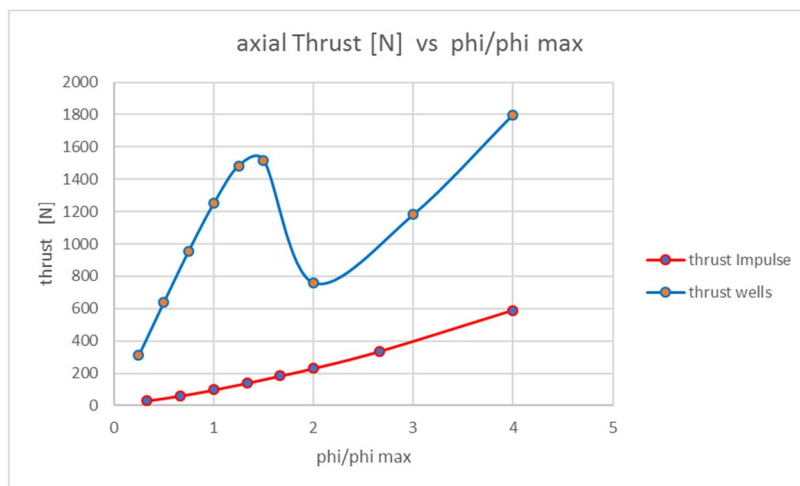

Fig. 4-6: Axial loads for the two turbines

Axial load is higher for Wells turbine, and it have big variations when ϕ_r changes, because of the stalling between 1.5 and 2; this suggests that under stalling, sudden oscillations in axial forces appear, giving a different behaviour towards fatigue than for Impulse turbine.

5 CONCLUSIONS:

In this work two wind self-rectifying turbines have been studied for a possible application in the Channel Tunnel: Wells turbine and Impulse turbine. A one dimensional model based on triangles of velocity and pressure drop correlations, and a two dimensional model based on CFD calculations with StarCCM+ have been developed to design the turbines given the specifications of the study case. Both the models are steady state, and calculations are performed at a mean radius.

After having designed the two turbines, a comparison between them is made, and it is shown that Impulse turbine is a better choice, because it has a broader range of applicability in which efficiency is not far from the design point one for a broad range of air flow velocities so that velocity control and power tracking is not as much as important as for Wells turbine. In Wells turbine the range of applicability is narrower, basically limited by occurring of stall; the stalling region in Wells turbine, moreover, doesn't permit self-starting. The fact that Impulse turbine operate with lower rotational velocities, then, implies that centrifugal forces on the blades are not as high as for Wells turbine, in which rotational velocities have to be maintained high not to lead to stall. Also axial loading are higher in the case of Wells turbine, so that more stress has to be sustained by the bearings.

In the future, the two models will be extended to full 3D analysis in steady state, and also unsteady state analysis will be performed, in order to deal with the flow transient phenomena that happens in the tunnels.

6 Bibliography

[1] F. Sabatier, "Réduction des apportes calorifiques dans les tunnels ferroviaires," 2015.

[2] K. K. S. T. R. S. Inoue M, "Simulation of starting characteristics of the Wells turbine," in *Proceedings of the AIAA/ASME 4th fluid mechanics, plasma dynamics and laser conference*, Atlanta, USA, 1986.

[3] S. T. K. K. I. M. Takao M, "Air turbine with self-pitch-controlled blades for wave energy conversion," *Int J Offshore Polar Eng,* vol. 7(4), p. 308–12., 1997.

[4] D. A. &. G. Mathieson, "An Examination of the Flow and Pressure Losses in Blade Rows of Axial Turbines," London, 1955.

[5] A. Howell, "The present basis of axial compressor design: Part 1, Casade theory and performance," vol. M, no. 2095, 1942.

[6] A. Howell, "Design of axial compressors," *Poceedings of the Institution of Mechanical Engineers,* 1945.

[7] A. Howell, "Flid dynamics of axial compressors," *Proceedings of the Institution of Mechanical Engineers,* 1945.

[8] X. L. Aamer Bilal Asghar, "Estimation of wind turbine power coefficient by adaptive neuro-fuzzy methodology," *Neurocomputing,* no. 238, 2017.

[9] M. T. Toshiaki Setoguchi, "Current status of self rectifying air turbines for wave energy conversion," *Energy conversion and management,* vol. 47, 2006.

[10] W. T. F. M. H. Boake CB, "Overview and initial operational experience of the LIMPET wave energy plant," in *Proceedings of the 12th international offshore and polar engineering conference.*, 2002.

[11] S. Raghunathan, "The Wells air Turbine for Wave Energy Conversion," *Progress in Aerospace Sciences,* vol. 31, 1995.

[12] J. C. H. Antonio F.O. Falcao, "Oscillating-water-column wave energy converters and air turbines: A review," *Renewable Energy,* no. 85, 2016.

[13] S. H. M. K. T.Setoguchi, "A review of Impulse turbines for wave energy conversion," *Renewable Energy,* vol. 23, 2001.

[14] T. S. K. K. S. M. M.Takao, "Noise characteristics of turbines for wave power conversion," *Proceedings of the institution of Mechanical Engineers,* vol. 216, 2002.

[18] S. T.Setoguchi, *Renewable Energy,* no. 23, 2001.